Swiss J Geosci (2010) 103:385–405
DOI 10.1007/s00015-010-0046-9

Alpine overdeepenings and paleo-ice flow changes: an integrated geophysical-sedimentological case study from Tyrol (Austria)

Jürgen M. Reitner · Wilfried Gruber · Alexander Römer · Rainer Morawetz

Received: 13 February 2008 / Accepted: 24 August 2010 / Published online: 1 December 2010

Abstract We present a study of the inneralpine basin of Hopfgarten focused on the analysis of basin fill in order to reveal its formation in relation to paleo-ice flow and tectonics. The study is based on geological mapping as well as seismic (reflection and refraction) and geoelectrical surveys. The oldest sequence in the basin, identified by seismic stratigraphy at 400 m below surface, consists of coarse grained sediments of supposedly Oligocene to Miocene age, which subsided along faults linked to the Inn fault. Three superimposed sequences, each displaying baselaps in contact with a subglacially formed unconformity and sigmoid foresets, show pleniglacial conditions followed by a glaciolacustrine environment. The uppermost of these three sequences lies on top of last glacial maximum till (LGM; Würmian Pleniglacial; MIS 2) and represents Termination I. The middle sequence is classified as Termination II following the Rissian Pleniglacial (MIS 6). The oldest glacial sequence cannot be constrained chronostratigraphically but might correlate with Termination V following the major glaciation of MIS 12. Limited glacial erosion during the LGM occurred only during the ice build-up phase. Further overdeepening was impeded due to topographic barrier and mutual blockades of glaciers within this highly dissected landscape. The occurrence and relative timing of the impediment was controlled by the onset of transfluences and thus by the altitude of coles. The higher amount of overdeepening during older glacial periods is explained by longer phases of free ice advance in the ice build up phase due to higher transfluences routes at that time. Thus, the preservation of older Pleistocene sequences within the basin may be the result of the lowering of watersheds from one glaciation to the next. Our model of an inverse relationship between glacial shaping of the surface and the subsurface may apply to similar Alpine landscapes as well.

Keywords Lithostratigraphy · Seismic stratigraphy · Glacial erosion · Glacier reconstruction · Landscape evolution · Integrated interpretation

Editorial handling: Markus Fiebig & Kurt Decker.

J. M. Reitner (✉) · A. Römer
Geologische Bundesanstalt, Neulinggasse 38,
1030 Vienna, Austria
e-mail: juergen.reitner@geologie.ac.at

A. Römer
e-mail: alexander.roemer@geologie.ac.at

W. Gruber
HOT Engineering, Parkstraße 8, 8700 Leoben, Austria
e-mail: wilfried.gruber@hoteng.com

R. Morawetz
Joanneum Research Forschungsgesellschaft m.b.H,
Roseggerstraße 17, 8700 Leoben, Austria
e-mail: rainer.morawetz@joanneum.at

Introduction

Estimates of the amount of subglacial erosion substantially rely on documents of the action of paleoglaciers especially in overdeepened valleys and basins. In the Alps, the first direct evidence of glacial overdeepening was revealed by a tragic tunneling project beneath the Swiss Gasterntal in 1908 (Schweizerische Bauzeitung, 1908: cit. in Schlüchter, 1983). But even drillings rarely document overdeepening since they are most often hydrogeologically motivated and do not reach down to the bedrock. Geophysical data however, especially seismic surveys of alpine and perialpine valleys, basins and lakes, are well suited to reveal basement depths of up to 1,000 m and can increase our

knowledge of overdeepened bedrock topography substantially (e.g. Finkh et al. 1984; Wildi 1984; Weber et al. 1990; Pfiffner et al. 1997). In combination with actualistic studies (e.g. Hooke 1991; Smith et al. 2007), this has led to a better understanding of the contributing processes such as erosion by basal ice and subglacial meltwater action.

Geophysical data also elucidate the structure of sediments in overdeepened inneralpine valleys, indicating a rapid infill by deltaic sediments (e.g. Burgschwaiger and Schmid 2001) and partly by mass movements originating from overdeepened slopes (e.g. Gruber and Weber 2004). In most cases, geophysical data accompanied by occasional drillings indicate a shaping of valleys during the last glacial maximum (LGM) and subsequent sedimentary filling during the following deglaciation (Termination I; van Husen 1979). There are some locations along inneralpine valley flanks showing deposits of Termination II and older (Grüger 1979; Drescher-Schneider 2000; Draxler 2000; Reitner and Draxler 2002), which is in accordance with the evidence of multiple glaciations in the southern as well as in the northern Alpine foreland (van Husen 2004 cf). However, in the Eastern Alps the initial valley formation by fluvial incision was linked to the morphogenesis driven by tectonical processes starting in the Paleocene and followed by major changes in drainage pattern during the Miocene (Frisch et al. 1998).

The impact of today's tectonic movements, expressed by shortening trends (e.g. Grenerczy et al. 2005), on the shaping of valleys during the quaternary is still a matter of debate. Indications of Oligocene to Miocene deposits at the bottom of overdeepened valleys along major strike slip faults, like the Inn valley, suggest tectonic subsidence linked to small-scale pull-apart basins (Poscher 1993). On the one hand, tectonically induced complex drainage systems with valley trains running across or oblique to the general ice flow, had a major impact on glacier flow and dynamics. On the other hand, glacial shaping and erosion apparently altered the topography resulting in the broadening of valley floors, oversteepening of flanks as well as in a successive lowering of water divides and thus ice transfluences routes for subsequent glaciations.

In this paper we present sedimentary and geophysical data of a small Alpine basin in order to address the following aspects:

1. The effect of a highly dissected mountain topography on ice dynamics in terms of promoting ice-build up as well as restricting erosion.
2. The limitations of paleo-glaciological models derived from the youngest sequence, in this case the LGM sequence, for explaining sedimentary remnants of older glaciations.
3. The combination between surface geology and geophysical data, especially seismic stratigraphy, for developing a climatostratigraphy.
4. The formation and shaping of a small basin in context of Alpine morphogenetic development.

Study area

Morphological and geological setting

The basin of Hopfgarten resembles the area around the village of Hopfgarten (622 m asl.) within the Kitzbüheler Alpen and is located around 10 km south–east of the Inn valley (village of Wörgl in Figs. 1, 2, 3). It is drained by the river Brixentaler Ache, a tributary of the river Inn. The main feeder rivers of the Brixentaler Ache are the rivers Windauer Ache and Kelchsauer Ache. Their drainage areas are surrounded by up to ~2,400 m high summits. Both valleys have cols in 1,686 and 1,983 m asl. (locations A and B in Figs. 1, 2), respectively, that connect them to the E–W trending Salzach valley, which drains the mountain chain of the Hohen Tauern with still glaciated summits and cirques.

The north-western edge of the Hopfgarten area consists of red sandstone (PSK), whereas carbonates of the Northern Calcareous Alps (NCA) occur west of Wörgl only on both Inn valley flanks (Ampferer and Ohnesorge 1918; Fig. 3). The largest part of the Kitzbüheler Alpen around Hopfgarten is made up of schists and metasandstones ("graywacke") of the Grauwackenzone (GWZ) and towards the south of quartzphyllite of the Innsbrucker Quarzphyllit Zone (Ampferer and Ohnesorge 1918; Heinisch and Panwitz 2007; Fig. 3). The latter two are summarised under the term 'GWZ' for reasons of simplicity.

Quaternary geology of the study area

The following description is based on Reitner (2005). Sedimentological logging of available sections was carried out according to standard approaches (Jones et al. 1999; Evans and Benn 2004) using a modified lithofacies classification of Keller (1996) based on Eyles et al. (1983) and Miall (1996).

In the basin of Hopfgarten terraces up to 150 m high (Figs. 3, 4) with different levels, which extend towards the tributary valleys of the Brixental, the Windau valley and the Kelchsau valley are found. They contain a tripartite sedimentary succession (unit A, B and C) which will be characterised in terms of lithofacies, sedimentary processes, paleoclimatological conditions and chronostratigraphy.

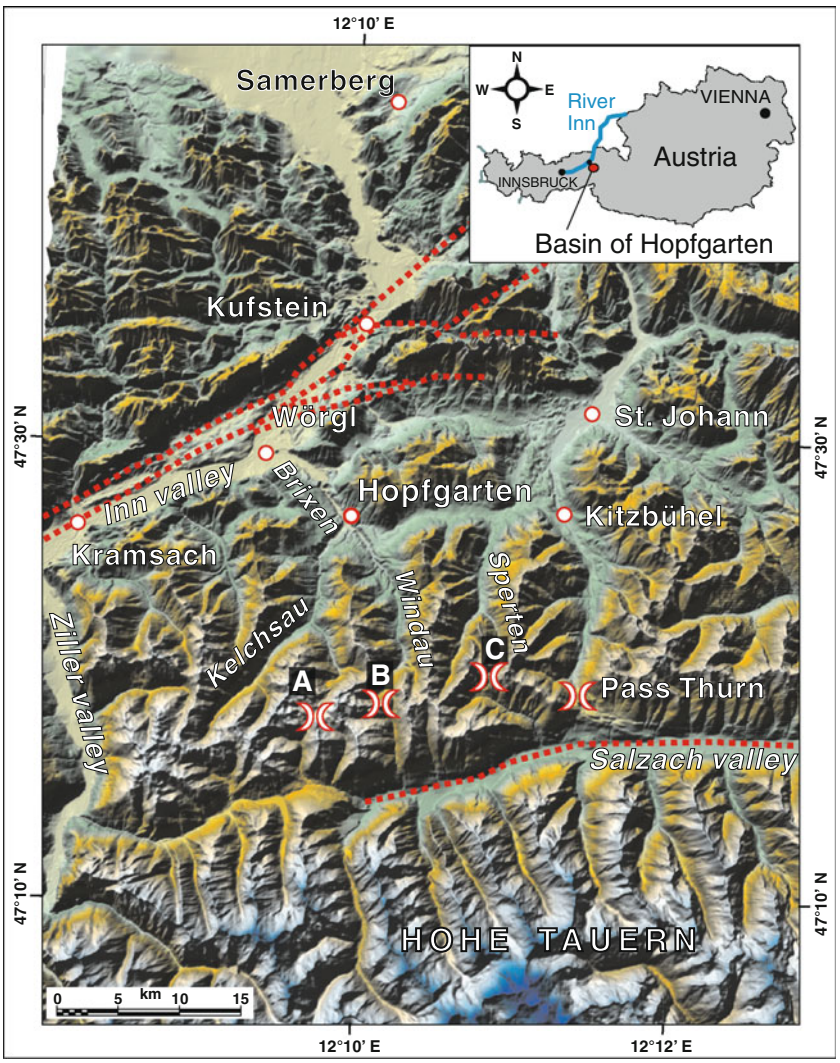

Fig. 1 Digital elevation model (DEM) with the location and morphology of the study area and its surroundings. Major faults related to Miocene tectonics are indicated (*dashed red lines*) based on Pestal et al. (2004). Bridge-symbols indicate the cols and former ice transfluences routes from the Salzach valley to *A* the Kelchsau valley in 1,983 m asl *B* the Windau valley in 1,686 m asl. and *C* the Sperten valley (Spertental) in 1,713 m asl. The most prominent similar feature is that of Pass Thurn (1,274 m asl.) towards the Kitzbühel valley

Special paleogeographical aspects will be considered in the following chapter.

The dominant lithofacies of the lowest *unit A* are horizontally bedded sheets of clast-supported, massive gravels, with clasts up to cobble size and occasionally recognizable imbrication (cGcm (i), for grain size distribution see Fig. 5). Small troughs filled with trough bed sand (St) or lenses of massive sand (Sm) are interbedded. These gravel sheets are interpreted as deposits of shallow braided rivers. The only local clast lithologies (GWZ) in combination with its occurrence in the tributary valleys point to a deposition by the precursors of modern rivers like Windauer Ache and the Kelchsauer Ache.

In some locations, mostly at the margin of the basin, organic bearing sediments and lignite are intercalated with the described coarse-grained lithofacies at different altitudes (Zailer 1910; Schulz and Fuchs 1991). This fine-grained subunit with a thickness of less than 10 m consists of coal (PC), laminated silts (Fl) and sand (Sm) partly with organic debris (Flo, Sho), and occasionally coarse-grained clasts to matrix supported diamicts (Dmm, Dcm). This facies association most probably displays sedimentary conditions of a backswamp-area with peat growth of overbank-sedimentation formed up-flow of alluvial fans impeding the drainage. Pollen-analyses indicate the arboreal environment during the early Würmian interstadials, the 1st and the 2nd, respectively (MIS 5c and 5a; Reitner and Draxler 2002). Thus, the braided river deposition most probably reflects the non arboreal climatic deterioration of the two early Würmian stadials, MIS 5d and 5b resulting in considerable aggradation (Reitner and Draxler 2002).

Unit A is overlain by a massive, matrix-supported and over-consolidated diamict (for grain size distribution see Fig. 5) with subangular to subrounded, frequently striated clasts and occasional indications of shear planes [Dmm (s)], *unit B*. Based on these macroscopic features and the even grain size distribution this diamicton was classified as a basal till, in the sense of "subglacial traction till" (Evans

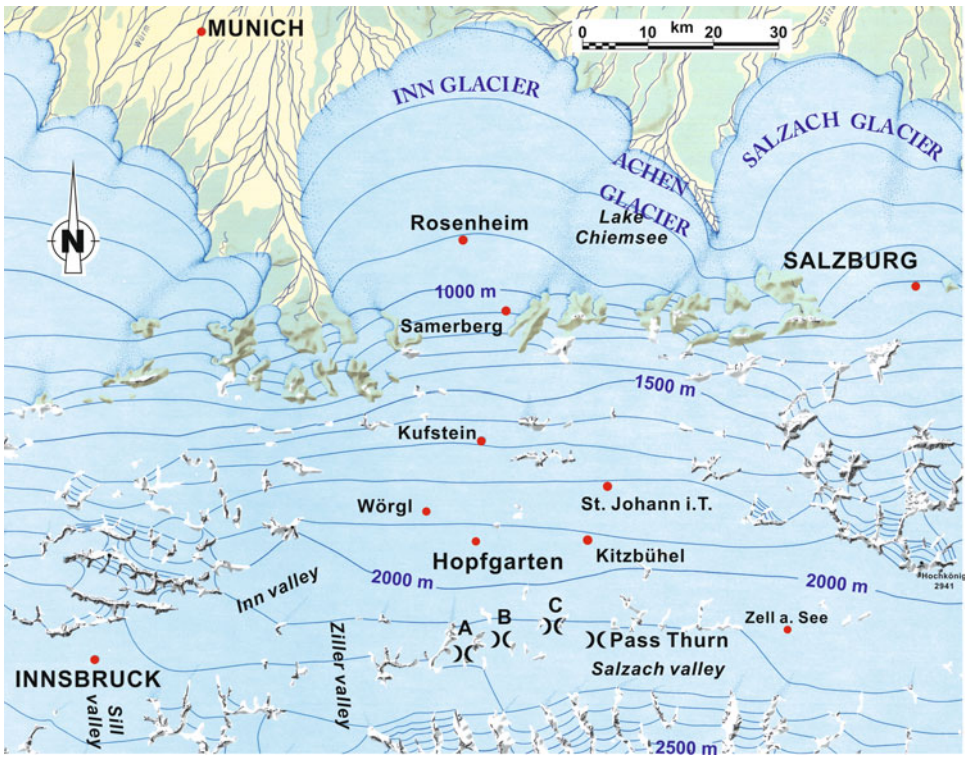

Fig. 2 The network of valley glaciers during the climax of the LGM after van Husen (1987). The position of the study area and other localities are indicated (for bridge-symbols see Fig. 1)

et al. 2006), and more specific that of "lodgement till" (Dreimanis1988). The contact between unit A and B is sharp and can be characterised in the large scale as a disconformity (definition after Bates and Jackson 1987), i.e. an unconformity in which the bedding planes above and below the breaks are essentially parallel. However, the basal till of *unit B* continues towards the flanks of the basin, where it covers big areas with a nonconformity contact (definition after Bates and Jackson 1987) on top of the basement rocks. In general the observed thickness of the basal till within the sediment sequence is between 2 and 10 m (like in the borehole west of Westendorf; Fig. 4b; Mostler 1993). Such diamictic sediments with erratic clast lithologies indicate a deposition by a glacier flowing from the Inn valley the Hopfgarten basin, which is commonly referred as the Inn glacier.

The clast lithology of the basal till (*unit B*) shows a significant change from the north-westernmost and, thus located closest to the Inn valley, part of the basin to the south–east. At the north-westernmost as well as the north-eastern locations (locations A, B and C in Fig. 3) high contents of clasts derived from the Inn valley drainage system. NCA limestone and dolomite clasts as well as crystalline rocks, are evident. The latter are e.g. a gneiss called Zentralgneis derived from the Hohen Tauern via the Ziller valley, an eclogite from the Ötz valley and amphibolites. It successively diminishes south of Hopfgarten towards the Windau valley (trend indicated from location D, to E and F in Fig. 3), where such erratic lithologies as well as amphibol-bearing micaschists ("Hornblendegarbenschiefer") and the indicator lithology of the Innglacier system, the Juliergranit (granite) can only be found in one location (location G in Fig. 3). This provenance from the Inn valley is displayed also in the clast fabric of the till at location E (Fig. 3). There a dominant NW–SE trend of the a-axis with a prevailing dip towards NW, also indicated by a shear plane, is present.

In general erratic boulders mostly of ZG-type are common on top of the erratic-clasts bearing *unit B* as well as on the bedrock surface. However, it is remarkable that ZG occurs in the upper Windau valley only as boulders but not in the basal till of the *unit B,* which contains only clasts of local provenience indicating a formation by a local glaciers descending from this valley.

The deposits of *unit C* show in general a tripartite, coarsening-upward delta sequence with a fine-grained bottomset, a foreset and finally a topset typical for Gilbert delta-sequence (Postma 1990). This delta-sequence conformably overlies the basal till of *unit B* and in most cases directly the lowest *unit A*. The latter contact may be classified as a paraconformity, i.e. an obscure or uncertain unconformity in which no erosion surface is discernable and in which the beds and above the break are parallel (definition after Bates and Jackson 1987).

The bottom set is up to 20 m thick and comprises massive and laminated silts (Fm, Fl) with occasional dropstones. The foreset beds consisting of planar-bedded gravels (Gcp) to gravel-sand mixtures (GSp), with intercalated ripple-bedded

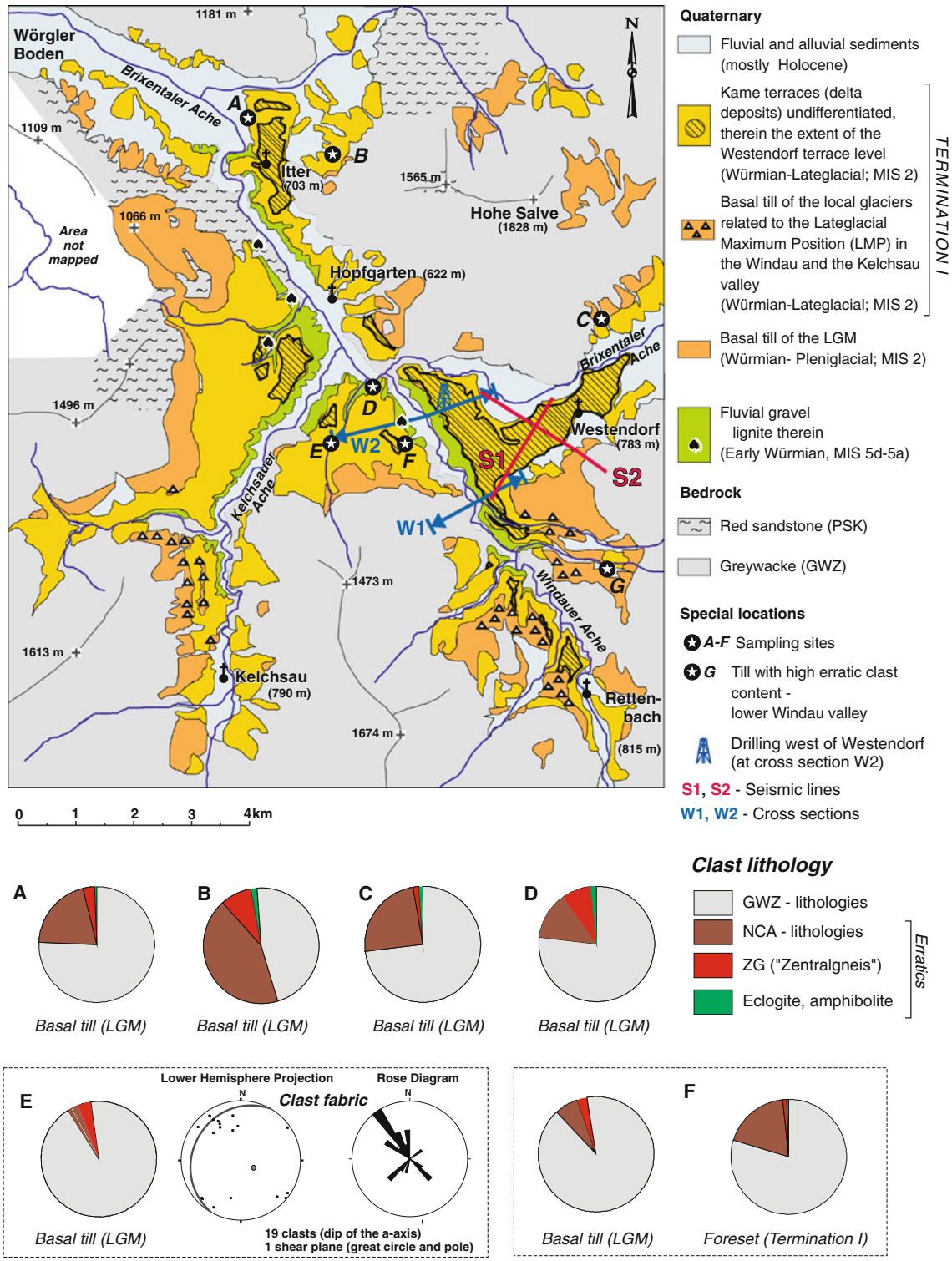

Fig. 3 Simplified geological map of the basin of Hopfgarten based on Reitner (2007) with special locations (**a**–**g**), the position of the *seismic lines* (S1, S2) and that of the cross sections (W1, W2)

(especially with climbing ripples) to massive Sands (Sr, Sm) show dips between 10° and 25°.

The occurrence of kettle holes, ice contact structures as well as the occasional preservation of striae in combination with ripple drift lamination, indicate rapid sedimentation of ice contact deltas, which in some cases are of Hjulström-type (Postma 1990) with missing gravelly clinoforms (Jopling and Walker 1968) as well. The final sedimentation

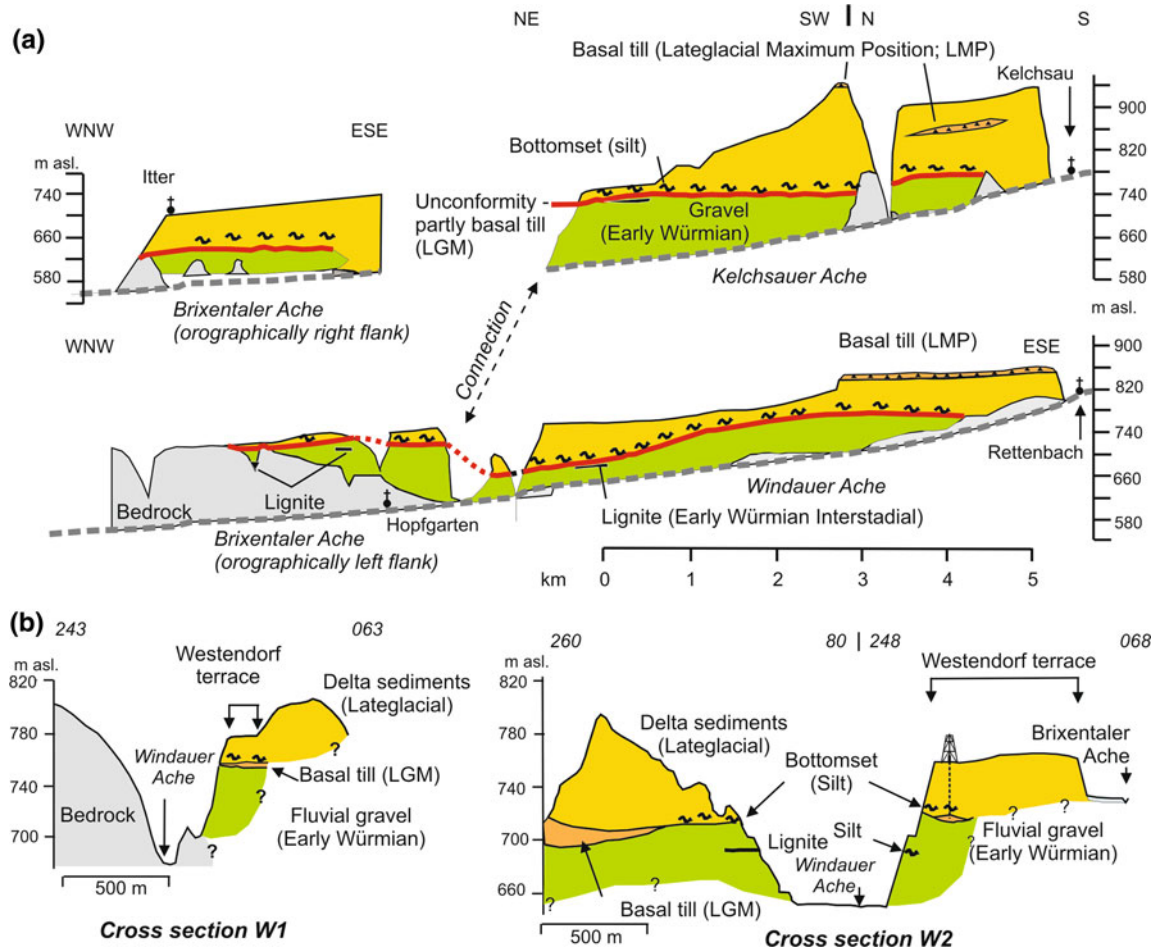

Fig. 4 **a** Geological sections along the rivers Brixentaler Ache, Windauer Ache and Kelchsauer Ache. **b** Geological cross sections W1 and W2 in the Windau valley (location see Fig. 3)

in the Hopfgarten basin and the formation of the prominent Westendorf terrace occurred when the front of the stagnant Inn glacier blocked the drainage of the whole basin at its north-western margin. All these features indicate a formation during the phase of early Lateglacial ice decay (Reitner 2007) and thus a document of the beginning of Termination I. Moreover, this classification is supported by a dating of Westendorf terrace sediments west of Hopfgarten with optically stimulated luminescence (OSL) with 18.7 ± 1.7 kyr BP (Klasen et al. 2007). Oscillations of local glacier towards their Lateglacial Maxium Position happened in this phase, which is indicated by the till of the lateglacial windau glacier on top of the kame terrace in the upper Windau valley (Figs. 3, 4). Consequently, the age of the basal till of *Unit B* is regarded as Würmian pleniglacial (LGM, MIS 2) as it is conformably superposed by the delta-sequence of Termination I, indicating only a change from the subglacial to the glaciolacustrine environment without any major hiatus.

In contrast, the unconformable contact between the LGM till (*unit B*) and the fluvial deposits of *unit A* in combination with the stratigraphic interpretation of the uppermost peat layer (MIS 5a) indicate that sediments of the Middle Würmian (MIS 4-3) and the advance phase of the LGM (MIS 2), which in total have a thickness of 100 m and more in the Inn valley (Fliri 1973) and its tributaries (e.g. Reitner 2008), are missing due to glacial erosion.

Ice flow pattern and glacial erosion during the LGM

Based upon the distribution of erratic clasts and boulders a branch of the Inn glacier advanced the Brixental valley upwards reaching Hopfgarten basin earlier than the local glaciers of the Windau and Kelchsau valleys. This dominance of the Inn glacier can be explained not only by its large accumulation area in places more than 3,000 m asl. but also by ice dynamical processes. According to van Husen (2000, 2004), the topography of the longitudinal valleys (such as the Inn and the Salzach valleys), especially in their relation to the tributary valleys, had a fundamental impact on the rate of ice build-up as well as on the glacier extent during the major glaciations. In the Inn valley, the

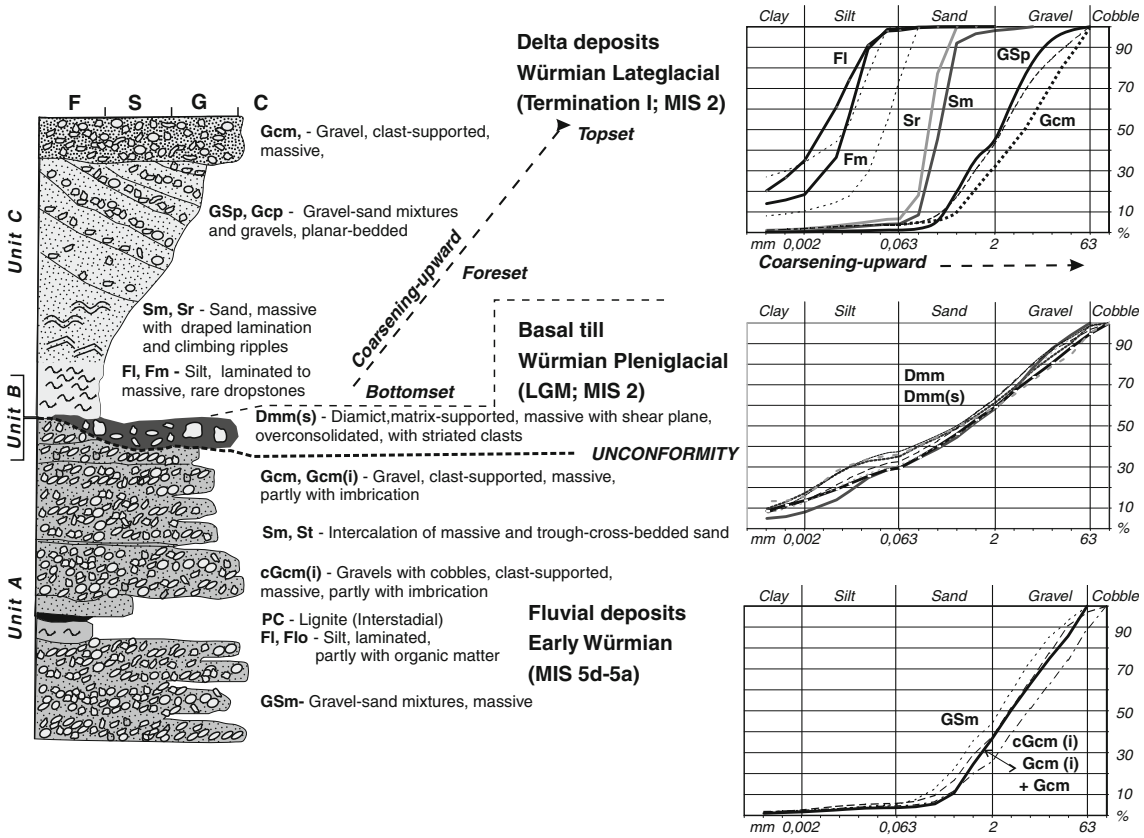

Fig. 5 Idealized lithological column of mapped units in the Hopfgarten area and selected grainsize curves

phase at the beginning of the LGM was characterised by ice congestion in the narrow Inn valley as a result of a strong inflow of ice, especially from the southern tributaries with large, high elevated drainage areas (e.g. Ziller valley, s. Fig. 2). As a consequence, the ice surface rose and a rapid expansion of the accumulation area occurred, favouring quick ice build-up. Due to this process, the Inn glacier as well as the Salzach glacier (s. Reitner 2005) could cross watersheds to the north before these valleys were filled with local ice.

Clast lithologies in the basal till like "Zentralgneis" and "Hornblendegarbenschiefer" support this model where ice from the Ziller valley (Zillertal), the easternmost tributary valley of the Inn valley that nowadays has still glaciated headwaters, form the eastern part of the Inn glacier system. The same is true for NCA-limestone and PSK which outcrop between the Ziller valley and the study area. Due to supposed strong ice input from this and other valleys eastward from Innsbruck, the occurrence of lithologies originating west of Innsbruck (eclogite, Julier granite) cannot be explained solely by transport via laminar ice flow. Subglacial erosion of proglacial fluvial gravels ("Vorstoßschotter") deposited in the Inn valley during the glacier advance at the start of the LGM (van Husen 2000, 2004) as well as that of older glacial deposits, seems to be a plausible reason thereof. In addition, transport by englacial and subglacial meltwater may have partially contributed to a mixing of lithologies.

In this early state of ice build-up Windau and Kelchsau glaciers were soon blocked in the lower section of their valleys (Fig. 6a). In the Windau valley the Inn glacier reached for a short time the location G (Fig. 3) as indicated by the erratic-rich till at that location.

In the course of the further advance phase (Fig. 6b) both local glaciers were forced to flow eastwards up the Brixental valley. Towards the east the Achen glacier of the Kitzbühel valley (also called Chiemsee glacier) received a strong inflow of ice from the high Hohen Tauern mountain chain via the low transfluence route of Pass Thurn (1,274 m) due to similar ice dynamical processes in the Salzach valley as described for the Inn valley (see above). This conclusion is based on clast analyses of basal tills (Reitner 2005). As a result the Achenglacier obstructed any flow east of Hopfgarten basin. Thus, the local glaciers of Hopfgarten area were also blocked in Brixental valley towards the east and were forced during further ice growth to overspill the up to 1,200 m high east–west trending chain east-northeast of Hopfgarten towards the north to north-east.

This principal pattern of glacier flow was most probably slightly modified in the course of further ice build-up due

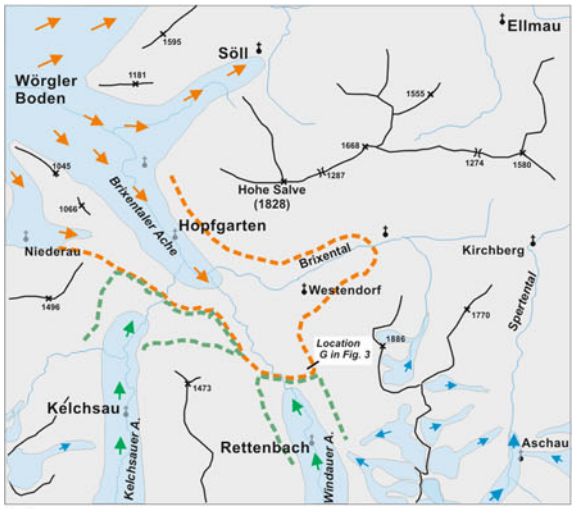

◀ **Fig. 6** Ice flow model from the ice build-up phase to the climax of the LGM. **a** Early ingression of the Inn glacier into the basin of Hopfgarten and early impediment of Windau and Kelchsau glacier (*dashed lines*). **b** Advanced phase of ice-build up with the blockade of ice flow towards the east by the Achen glacier. **c** Ice flow during the climax of the LGM, when the ice transfluences (locations *A* and *B* in Figs. 1, 2) from the Salzach valley to the Windau and Kelchsau valley were active. Ice surface around Hopfgarten in 1,900 m asl

to successive onsets of ice transfluence (~1,700–2,000 m asl.; Fig. 1) from the Salzach valley, and thus from the Hohen Tauern towards the Windau, Kelchsau and other tributary valleys (Fig. 6c). The occurrence of Zentralgneis, the indicator lithology from the Hohen Tauern, in the upper valleys of Windau and Kelchsau only as big boulders on the surface of the basal till of LGM age but not within the subglacial sediment, seems to be surprising in this context. This finding is interpreted in terms of the local valley glaciers having already filled up the valleys and having been too dominant to allow subglacial transport by ice from the south. Thus, the erratic boulders were transported supra- to englacially prior to deposition. This model of a later enhancement of the glaciers in the Windau and Kelchsau valley implies that the distribution of the erratics within the basal till dominantly represents an early phase of ice build-up. The preserved structural elements within the lodgement till at location E (Fig. 3), such as the *a*-axis of the clasts and shear planes orientation dominantly dipping towards NW, both indicate a formation by a temperate Inn glacier which advanced towards SE.

The presented sedimentary evidence is in general accordance with the large scale reconstruction of the climax of the LGM around 24–21.5 kyr cal BP (Preusser 2004) which was at the time when the Inn glacier as the biggest one in the Eastern Alps, was connected with other Alpine glaciers and formed a network ("Eisstromnetzwerk"; van Husen 1987; Fig. 2) in the sense of transection glaciers (Benn and Evans 1998). In this phase the ice surface of this glacier network showed a decline from 2,200 to 2,100 m asl. in the Salzach valley in the south to ~1,900 m asl. at Hopfgarten. Hence, a consequent ice flow with a gradient in the range of 1° towards north and north-east, respectively, across the longitudinal and smaller E–W trending valleys (Salzach Brixental valleys) was thus independent from the existing fluvial drainage. During this phase wet based glacier conditions can generally be assumed on the basis of the occurrence of "subglacial traction till" (according to Evans et al. 2006) from the valley floors to nearly up to the higher valley flanks as well as the presence of drumlins in the larger valleys (lower Inn valley, area of Kitzbühel; Reitner 2005; Gruber et al. 2009).

According to this ice flow model, the preservation of pre-LGM sediments well above the modern valley floor throughout the whole Hopfgarten basin, or in other words, the lack of glacial overdeepening during the LGM, seems to be the result of a combination of following factors: the mutual blockade of local glaciers between the dominant glaciers, the Inn glacier to the west and the Achen glacier to the east, at the beginning of the LGM and the effect of a E–W trending basement barrier north to north-east of Hopfgarten during the climax of the LGM.

The major basal unconformity at the base of the LGM till shows a quite even geometry (Fig. 4a) without any indication of channel-like structures along all the valley flanks. Hence, this feature displays limited erosion by the flow of a temperate glacier and no linear incision by subglacial meltwater in the sense of a Nye-channel (Menzies 1995) as is typically found in the large scale "tunnel valleys" (e.g. Kristensen et al. 2007). It is inferred that the major part of sediment evacuation at the glacier base occurred during the earliest phase of ice build-up, when glacier advance was possible until the occurrence of various mutual impediments of (local) glacier flow (Fig. 6b). According to the preservation of till with an erratic distribution and a till fabric mirroring such a situation, the state of erosion soon got "frozen" due to the sealing of the basal unconformity by the superposing subglacial sediment. One key to understanding the supposed "non-erosion" at the climax of the LGM in the Hopfgarten basin might be seen in a combination of topography and subglacial hydraulics. According to the Alley et al. (2003) model the overdeepening process relies on the efficiency of sediment evacuation by pressurized subglacial meltwater. If we consider the northward ice flow upward and across the E–W trending rock barrier north to north-east of Hopfgarten, such that subglacial water may have been forced to flow upstream, a decompression of the water close to the pressure melting point would have resulted in supercooling of water and ice growth and consequently in the cessation of erosion at the glacier base. In the large scale, this situation could have led to the development of a wedge of quite immobile, maybe cold ice sticking to the toe of the slope, which successively extended southward into the centre of the basin. According to this hypothesis, the further northward ice flow occurred only at levels quite above the glacier base due to ice deformation resulting in no impact on basal erosion within the basin.

Methodology

Seismic methods

Seismic surveys were performed for geothermal exploration north–west of the village Westendorf (Fig. 7; Gruber et al. 2004). Data acquisition along two perpendicular lines, S1 and S2, utilized a dynamite source and a spread of 200 active recording channels in 10 m spacing. The methodological clue of the study is to seamlessly join together seismic reflection information from the deeper part with high fold seismic refraction analysis from in the uppermost tens of meters.

Seismic refraction processing utilized a subset of every 3rd to 5th shot gather. Thus, semi-automatically derived travel time curves densely cover the survey and subsequent

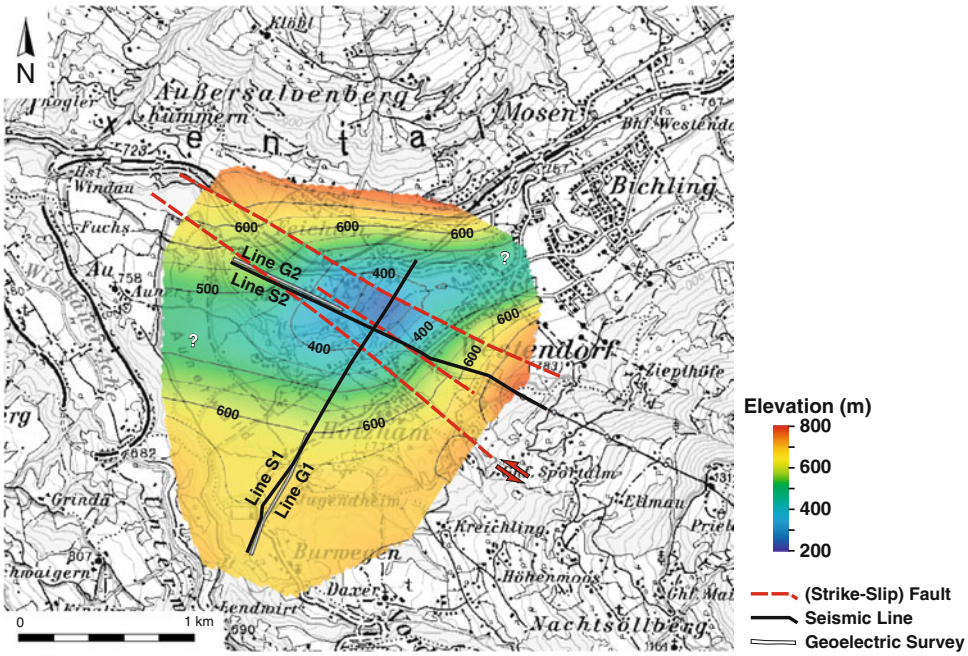

Fig. 7 Location of geophysical surveys and depth structure map of interpreted top of basement

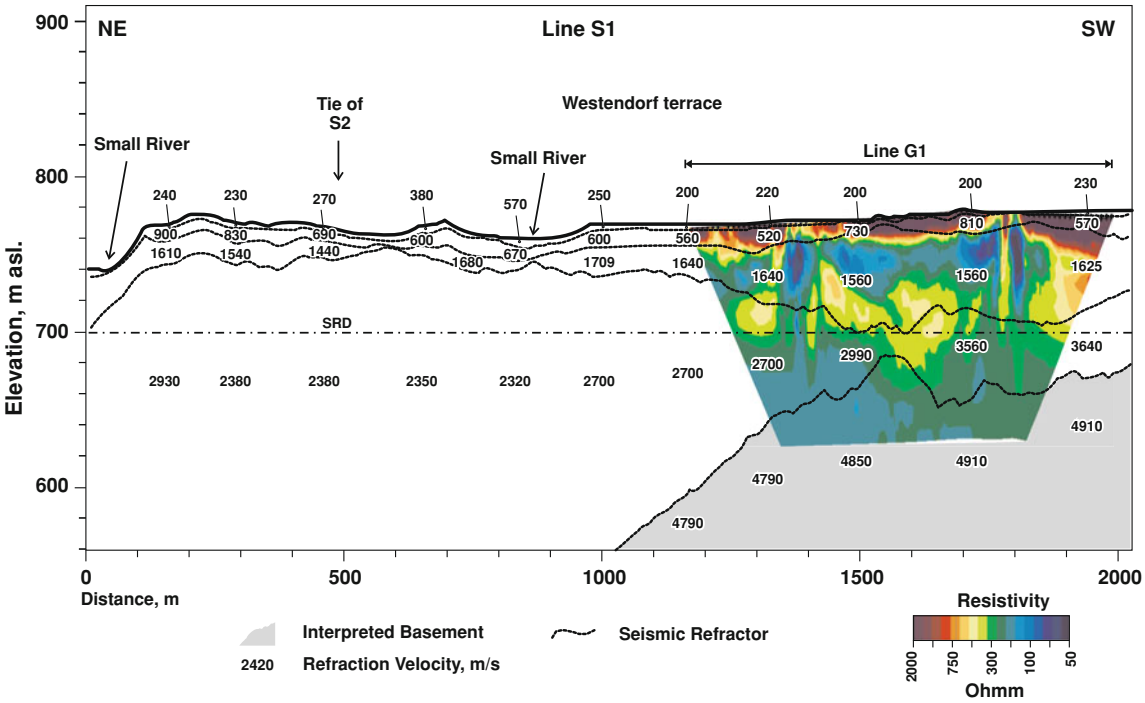

Fig. 8 Layer model derived from seismic refraction analysis along S1 and resistivity section G1. *Numbers* denote refraction velocities in m/s

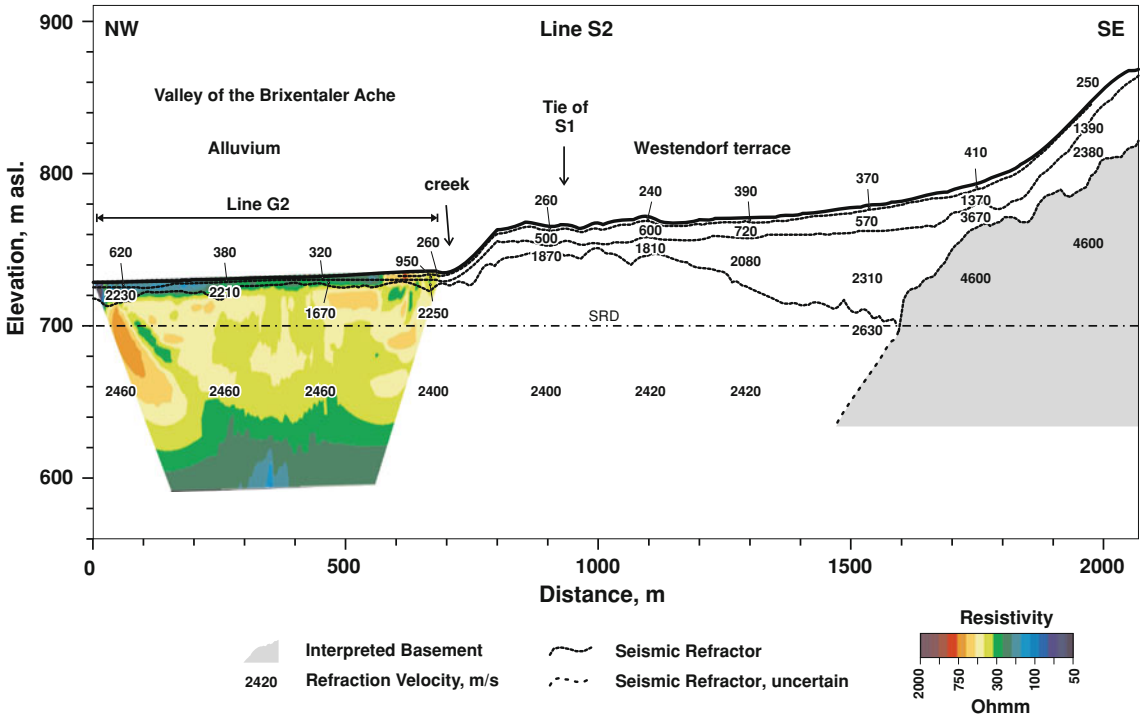

Fig. 9 Layer model derived from seismic refraction analysis along S2 and resistivity section inserted. *Numbers* are refraction velocities in m/s

refractor analysis is of high lateral resolution compared to classic seismic refraction surveys. Application of the generalized reciprocal method (GRM; Palmer 1980) generated sections in depth domain showing layers of contrasting seismic velocities (Figs. 8, 9).

Reflection data processing followed standard routines (Clearbout 1976; Yilmaz 1987). Careful manual trace editing and spectral whitening prior to spiking deconvolution were key operations to maintain results with good resolution and low noise. Static corrections were calculated

from the refraction seismic layer model, dynamic corrections are based on manually picked velocity models. Bandpass filtering and finite difference migration were applied to stacked sections. On resulting seismic time sections positive reflections denote interfaces with downward increase of acoustic impedance.

For time to depth conversion, seismic interval velocities from refraction analysis and stacking velocities from processing, were analyzed. Stacking velocities are found to be slightly lower than the refraction velocities. The lower velocities were preferred for construction of a V0-k velocity model (Slotnik 1936) to get a conservative result (shallow basin). For sedimentary rocks an intercept velocity of 1,950 m/s at the seismic reference datum of 700 m asl. and a gradient (velocity increase with depth) of 2.5 m/s per ms was derived, a constant velocity of 4,000 m/s was assigned to the bedrock. This model was used to convert the entire seismic time sections into depth domain to enable a joint interpretation with refraction and electric data.

Structural seismic interpretation investigated the layering and depth of sedimentary strata in the Hopfgarten basin. During sedimentological interpretation, reflection terminations and internal configuration are attributed to sedimentary features. Petrophysical parameters, the rock type and depositional environment of individual strata were established (Brown 2004).

Geoelectric survey

A multi-electrode geoelectrical survey was carried out to backup interpretation of the seismic results. Two geoelectric profiles were investigated; profile G1 at the soth-western part of seismic line S1 and profile G2 at the north-western end of seismic line S2 (Fig. 7). These profile locations were chosen to obtain additional information of possible shallow bedrock (depth <200 m). The lengths of the profiles are 830 m (G1) and 710 m (G2), both with an electrode spacing of 10 m. The use of Wenner-Schlumberger arrays resulted in an estimated investigation depth of 150–180 m.

Geoelectric data processing utilized an inversion based on the smoothness-constrained least-squares method including a topographic correction (Sasaki 1992; Oldenburg and Li 1994). Results are two 2D resistivity depth sections (Figs. 8, 9). Despite careful editing and removal of noise bursts on G1 still some perturbation is present from paved roads crossings.

Geophysics

Seismic refraction interpretation

Subsurface models from seismic refraction (Figs. 8, 9) analysis give details of the stratigraphy in the upper 200 m below the surface. In areas with good data coverage single layers were traced below this limit but with higher methodical uncertainty.

The deepest and thus fastest refractor identified is caused by the strong increase of refraction velocities to 4,700–4,900 m/s beneath generally lower velocity layers. It shows clear northward dips along the southern parts of both profiles until it vanishes in greater depth (near the centre of the profiles). In the south-western part of S1 the horizon flattens and shows a significant relief of up to 30 m. The existence of a southward dipping segment is uncertain at the north-eastern end of S1 below 500 m asl.

The shallower part of the refraction model consists of thin layers with a stepwise increase in velocities with depth. The uppermost layer is 3 m thick at maximum and its base follows the topography. Velocities are generally less than 380 m/s. The layer underneath is characterized by velocities from 500 to 800 m/s and thicknesses from 10 to 20 m. It occurs only inside the terrace and is missing in alluvial areas in the north of both profiles. The velocity increases to 1,370 m/s at the slope in the south–east of S2. The following layer (velocities of 1,440 to 1,800 m/s) significantly thickens to more than 60 m in the southern parts; also velocities increase to >2,300 m/s at the valley flank in the south–east.

The lowermost interval is a thick package of rock of uniform velocity between 2,300 and 2,700 m/s. While on seismic reflection data individual reflection patterns are seen in this interval no velocity contrast is identifiable. Only in the south-eastern part of S2 above the interpreted bedrock, velocities laterally increase to around 3,600 m/s.

Seismic reflection interpretation

Seismic reflection sections (Figs. 10, 11) were described by intervals of characteristic facies. Five individual seismic facies were identified:

Seismic facies F1 is dominated by fragments of weak sub-horizontal reflections. Amplitudes are increased locally and frequencies are generally low. Reflection continuity is low, often caused by intersections of steeply dipping high frequency reflections. Facies F1 occurs solely beneath the deepest, strongest, vertically dislocated reflection event on both sections. Seismofacies F1 is interpreted as response from bedrock.

Seismic facies F2 is characterised by low amplitude reflections that vary across the facies body. The central parts of the facies body are seismically nearly transparent and form a chaotic pattern of short reflections. The margins of the facies body are well defined by more continuous, sub-parallel events which onlap onto the strong reflectors underneath. Frequency content is higher than in F1. Facies F2 is limited to the deeper intervals (500–300 m asl.) in the

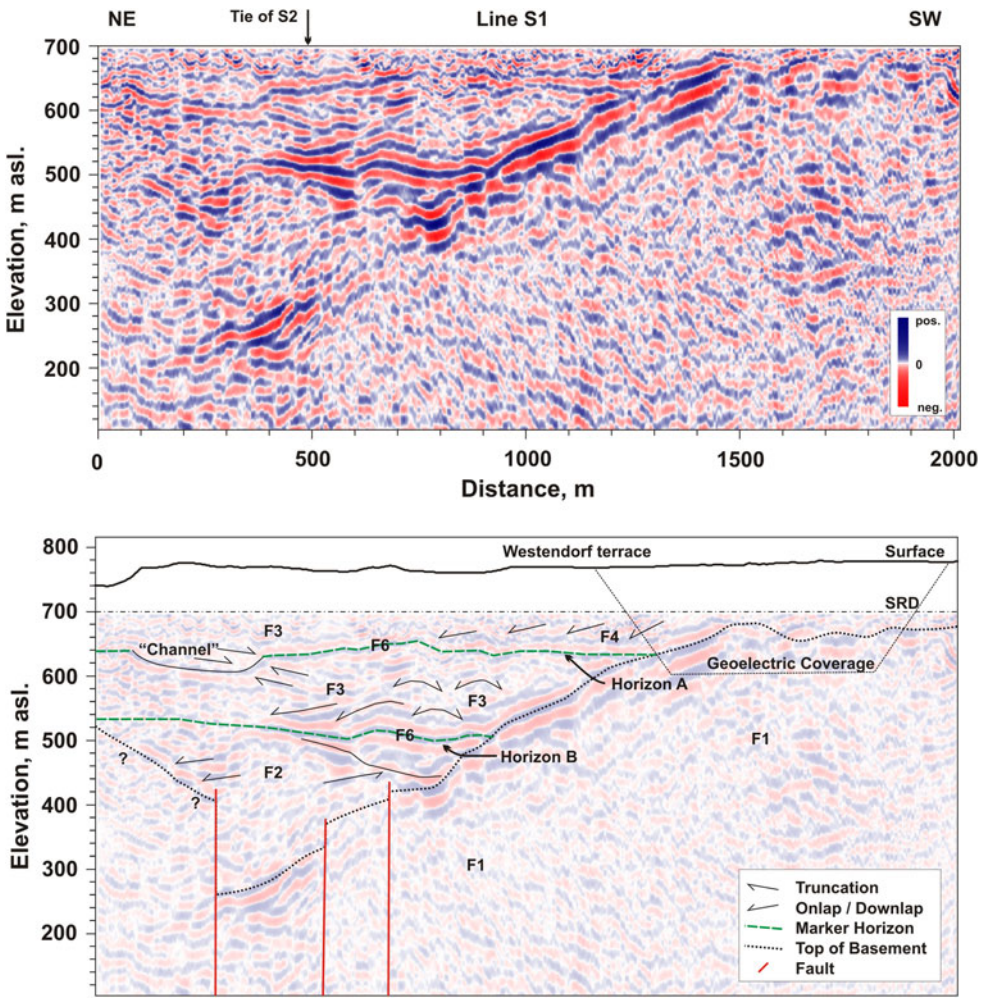

Fig. 10 Seismic reflection data of line S1 and interpretation of the migrated and depth-converted stack

central part of S2 and the north-eastern part of S1. Such facies are most likely generated by poorly stratified deposits which are coarse grained in general. A higher energy fluvial setting (braid plain deposits) is interpreted. Towards the margins of the facies, body energy was probably reduced resulting in finer grained interlayers generating subhorizontally onlapping reflections.

Seismic facies F3 typically consists of a series of sub-horizontal to gently tilted reflections turning laterally into clinoforms with downlaps pointing to northern directions. The same facies also appears as mounded events with downlaps on either side. Reflections are rather continuous and of medium strength and frequency. The bigger part of both sections can be described by this facies which can be related to coarse deltaic fore- and topsets. Clinoform and baselap geometry points to progradation towards northern directions. The twofold appearance of facies F3 (clino-forms and mounds) is thought to indicate the relation between the course of the section and the direction of deposition.

Seismic facies F4 can be described as a series of strongly dipping parallel reflections. They are of medium amplitude, continuous and predominantly downlap to the north. F4 is identified in the southern parts of both sections where it laterally grades into facies F3. Based on geometry and relation to basement facies F4 could be interpreted as alluvial fan or fan delta deposits. They are likely to grade into fluvio-deltaic sediments laterally.

Seismic facies F5 is an assemblage of strong horizontal parallel reflections. They are laterally persistent and of high frequency in the shallow parts. Reflection terminations are clear onlaps. Lower frequencies, probably due to damping are seen in deeper parts of the survey. Such seismic pattern is typically interpreted as parallel layered, fine grained sediments. These form bottomsets in the distal parts of a delta and low energy lacustrine settings.

Seismic facies F6 characteristics are low frequency signals of strong amplitude. They form sub-horizontal to undulating events across major parts of the sections. Thickness is often less than a single positive reflection, locally accompanied by negative lobes above and below. F6 obviously splits seismofacies packages by forming stratigraphically significant boundaries. These are picked as unconformities (Horizons A and B at about 500 and

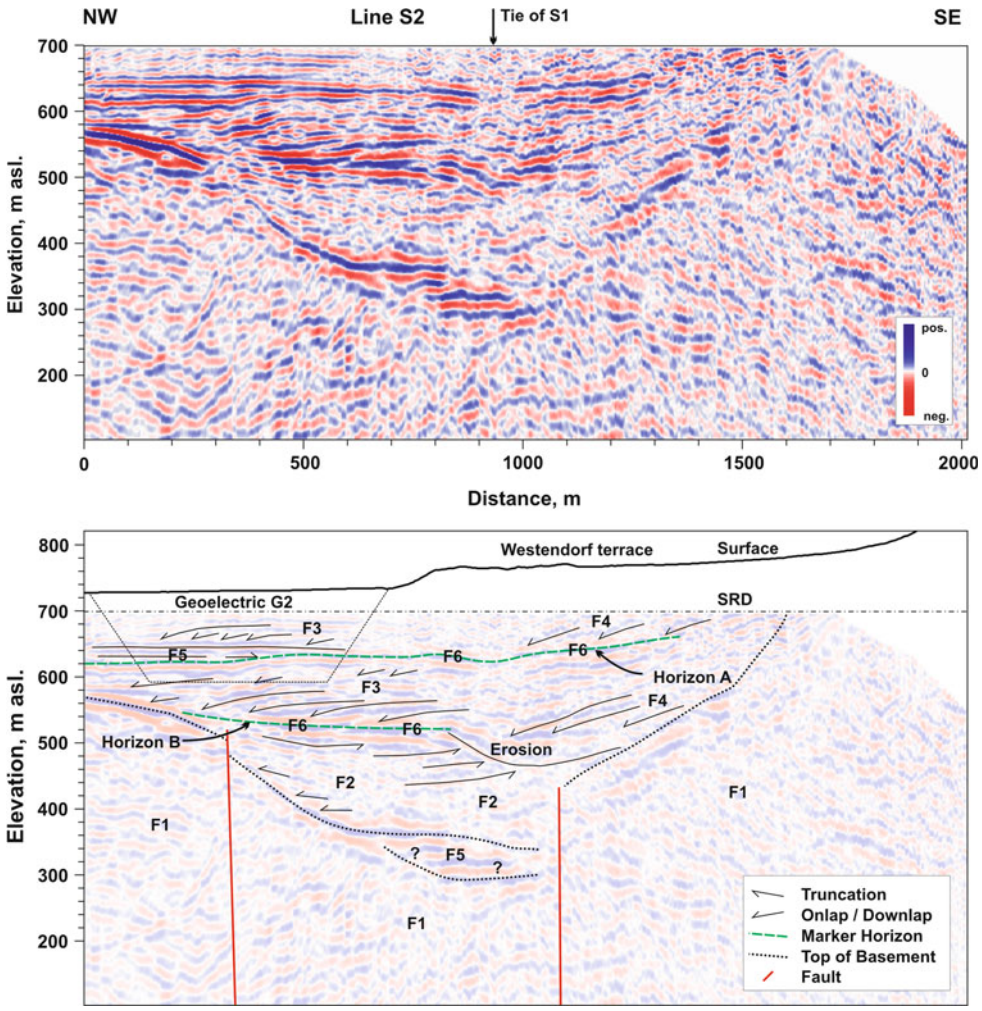

Fig. 11 Seismic reflection data of line S2, migrated and depth-converted stack and the interpretation on seismic patterns

630 m) that divide the sequence into a deep, middle and shallow sedimentary package. Single high amplitude reflectors are quite common in glacial settings (Pfiffner et al. 1997). They point to a thin layer of high acoustic contrast, probably due to significant compaction. These key horizons are interpreted as surfaces due to combined subglacial erosion and sedimentation containing basal till.

Geoelectric data interpretation

Along most parts of G2 (Fig. 9) a very thin layer (about 10 m) of relatively low electrical resistivity (200–300 Ω) is present, which thins out at 580 m near the south-eastern end. Underneath, relatively uniform resistivity range of 400–600 Ω make up a layer of at least 100 m thickness. It is underlain by rocks of minor resistivity <250 Ω, which reach to a maximal depth of 150 m (577 m asl.).

In contrast to G2 the topmost layer in G1 (Fig. 8) is characterized by a very high resistivity (>2,000 Ω). It has a thickness of 10–15 m and increases up to 30 m at the beginning of the profile in SW. Below that, a low resistivity layer (150–200 Ω) with a thickness of 20–30 m is observed, which is absent along the first 130 m in the SW. The results around 1,400 and 1,800 m were ignored during interpretation as data are disturbed from road crossings. The layer below about 740 m asl. shows resistivities around 400 Ω, laterally decreasing to 250–300 Ω with increasing thickness in the south-western part of the profile (profile meter: 1,700–2,000 m). The lowermost part is characterized by resistivities <200 Ω to the depth of 180 m (593 m asl.).

Discussion of results

Bedrock morphology

Bedrock ("graywacke" of the GWZ) is identified by seismic facies F1, refraction velocities greater than 4,700 m/s and medium resistivity of 250 Ω.

The top of the bedrock is correlated to the deepest strong positive seismic reflection, which is identifiable along most parts of the sections. Such strong reflections are likely at (methamorphic) basement-sediment interfaces caused by the large velocity contrast between these rocks. Similar results are also reported from seismic sections in the Rhone valley (Switzerland; Pfiffner et al. 1997).

At the southern ends of both profiles, the reflection decreases in amplitude and continuity when it approaches the surface. This may show the methodical limit of seismic reflection surveys to map shallow strata. However, refraction and electric data generally reveal high confidence bedrock interpretations.

At the south-western end of the profile shallow basement (about 500 asl.) is likely due to nearby outcrops but not clearly confirmed from geophysical surveys. In the north-eastern part of S1 just short segments of weak reflections can be found at depth below 400 m. Visibility of the bedrock reflector along the first 300 m of the profile is maybe reduced due to lower data coverage. Towards the centre of the section individual segments are vertically displaced against each other denoting faulted basement. The change in character between 500 and 700 m (profile length) is probably due to less seismic response from a structurally complex zone. Correlation at the line-tie to S2 gives way for two alternative interpretations (Fig. 11) in the central parts of the survey. Line S2 shows a continuous reflection forming a bowl-like structure.

The Hopfgarten basin is interpreted as a nearly 500 m deep west-east elongated structure (Fig. 7). It is open to the east and north–west while steep margins are constructed in the north and south–east (Fig. 7). The depocentre is dissected by a NW–SE oriented faultzone which follows roughly the valley of Brixental. Such a finding is in agreement with the occurrence of dominant NW–SE trending lineaments in the study area, like the lower valley of the Brixentaler Ache and that of the Windauer Ache (Figs. 1, 3). This trend is evident in the brittle faults south of Westendorf (Heinisch 2003) as well as in a halfgraben structure SW of Hopfgarten showing at least an up to 500 m subsidence of Permoskythian rocks (Heinisch 2005). Such structures supposedly may be linked as antithetic Riedel shears to the Inn fault (A. Gruber, pers. comm.). However, the structural elements point to a tectonic genesis of the Hopfgarten basin accompanied by relative subsidence, a situation which is also indicated in the Inn valley (see Preusser et al. 2010).

Combined sedimentological–geophysical model

A model of the sedimentary deposits of the Hopfgarten basin was synthesized from integrated interpretation of the geophysical and outcrop data presented above. The description of individual layers begins from the surface down to the bedrock as information and accuracy decrease with depth.

The clearly defined morphological and sedimentological situation on top of the Westendorf terrace, a result of the beginning of Termination I, is well mirrored in the results of the shallow geophysics. The lowest refraction velocities are generally caused by the thin (a few meters) weathering layer and display the general surface trend of the terrace including the undulating part (NE—part of profile S1 and middle part of profile S2) typical for kettle holes and hummocky terrain as a result of ice decay.

According to refraction line S1 on top of the Westendorf terrace, an upper sediment layer with a thickness trend from 30 m in the north to approx. 60 m towards the southern parts can be deciphered. At its very south-western end the base of this layer starts getting shallower again. Continuing this trend about 100 m off the seismic line leads to a mapped section showing a coarsening-upwards from a silty bottomset, to sandy-gravelly foreset and finally topset, typical for deposits of the Termination I (Würmian Lateglacial, *unit C*). High resistivities in the uppermost part of profile G1 correlate with low refraction velocities (600–800 m/s) and denote the well drained dry topset part of the terrace. On the one hand, the higher velocities (1,400–1,600 m/s) of the lower part of this layer might reflect the water saturation of the sand-gravel mixture of the foresets. On the other hand, such seismic units can be interpreted as glaciolacustrine fine-grained sediments (Büker et al. 1998). The downward trend into a low resistivity layer in the undisturbed central part of profile G1 supports the latter possibility and also points to a silty bottomset of the deltaic infill. Small differences between the results of the refraction seismics and the geoelectrics can be most likely put down to a slightly different run of both surveys. In general, thickness variations of the glaciolacustrine sediments are not surprising according to outcrop data which show this fine grained sediment sometimes accompanied with natural springs.

In principal, the Westendorf terrace part of S2 shows, according to the velocities, the same trend with a sandy gravelly layer as that of the line S1. However, two special situations are recorded at both ends:

Higher refraction velocities in the range of >4,000 m/s denote rocks different from those of the loose sediments of the terrace as illustrated. However, in the south-eastern end of S2 the velocity decrease at the slope towards the surface does not show a cover of loose sediments on top of basement rocks. In combination with the results of the geological mapping this is interpreted to reflect the increased disintegration of a rock due to a creeping mass movement.

At the north-western end of S2 in the area of the Brixental valley, a layer with velocities around 2,200 m/s

corresponds with low resistivity. It is just a few meters thick and thus probably not resolved across the entire survey. If we consider the outcrops along the Windau valley as well as the nearby drilling west of Westendorf (Fig. 4), this layer can be correlated with laminated silts of the bottomset occurring at the base of *unit C*. A thin layer of the underlying *unit B*, basal till of LGM age, may contribute to the higher velocities as well according to geophysical investigations supported by drillings in similar basins (Büker et al. 1998; Nitsche et al. 2001).

In general, shallow geophysics show the continuation of the outcrop situation with the uppermost sequence containing deltaic sediments (topset, foreset, bottomset) of *unit C* (Termination I) on top of the LGM till (*unit B*).

The top of the following sequence is identified by an increase of refraction velocity, indicating a higher degree of consolidation. The trend from relatively high resistivities to low ones of the geolelectric survey G2 down to the base of resolution again indicates a coarsening upward trend. Based on a comparison with results of a geoelectric survey on top of a deeply incised terrace SW of Hopfgarten (Reitner 2005), the resistivities between 710 m and 640 m asl. should display the sandy gravels, overwhelmingly that of the Early Würmian (*unit A*, MIS 5d-5a). Higher velocities in this horizon are explained with a dense packing due to consolidation, which seems to be responsible for a surprisingly high slope stability with near vertical scarps in the outcrops as well. The uppermost part (650 m to 700 m asl.) of the seismic reflection data in the north-western part of S2 with parallel reflections and subtle downlaps (facies F3) are correlated with the gravel-sheets of *unit A*. Downlaps, typical for F3 and F4 in the southern parts of the sections are regarded to show the progradation of alluvial fan deposits infilled from southern directions. The base of the upper gravelly layer is clearly formed by a set of onlapping parallel reflections (facies F5) on top of the prominent reflector "horizon A". This situation nicely correlates with a decrease in resistivity at G2 in the north–west of S2. Thus, this lower stratum most likely resembles a (silty) bottomset, which can reach a thickness of up to 40 m. Comparable seismic facies seen in lake deposits of the French Alps was interpreted as basin floor fan deposits (van Rensbergen et al. 1999). In this context of a lake infill, the slightly inclined downlaps (facies F3) directly on top of the bottomset in the north-western part of S2 in 650 m asl. are regarded as clinoforms of a prograding shoal water fan delta (Hjulström delta; Postma 1990).

In summary, this second sequence (from the top) shows a coarsening-upward trend. The occurrence of Early Würmian gravel well below the modern valley floor of the Brixental valley is not surprising if we consider the nowadays existence of an epigenetic valley cut into the bedrock downstream, leading to a higher local base level. However, the clinoforms below as indicated by the reflexion seismics have not been recognized along the lowest part of the Windau valley, maybe because of poor outcrops below approx. 650 m asl. The same is true for the fine-grained sediments of horizon A, which overwhelmingly should occur below the sole of the Windau valley.

The higher velocities around 3,000 m/s in the south-western-most part of section S1, clearly differ from that of the bedrock and the loose sediments are elusive regarding to their interpretation. One possible explanation for that would be the occurrence of again a disintegrated bedrock slope due to a mass movement.

In general, the geophysics again show a coarsening-upward sequence on top of an erosional surface (horizon A), with clinoforms and finally horizontal gravels. This surface of horizon A and facies F6 with only some undulations is attributed to subglacial erosion by ice flow. Hence, the channel-like feature at the north–east of S1, incised in the lower strata most probably points to linear subglacial meltwater action in the sense of a Nye-channel (Menzies 1995). Laterally widespread, strong reflections from facies F6 are interpreted as basal tills (Pfiffner et al. 1997). Like in the example above, the sedimentary sequence is inferred to have started at the beginning of a termination.

The sequence below horizon A is interpreted again as delta deposits prograding to north–west (sigmoid and baselaps) with an upward and north–westward decrease in slope angles indicating a transition into a more proximal environment. But undoubtable indications of horizontally layered topset strata, like in the sequence above, are missing. Same facies F3 shows a mounded pattern along S1, which is typical for a section across foresets in direction perpendicular to the progradation. The south-eastern part consisting of facies F4 (downlapping tilted reflections) is interpreted as alluvial fan, also infilled from south–east. Steep foreset slopes of up to 15° were analyzed, which point to coarse grained sediments that maintain such angles of repose. It is probably the equivalent to the recent mass movement discussed above. Structures indicating sediment transport from nearby northern valley flanks have not been identified so far.

The package mentioned before is underlaid by the prominent "horizon B" (facies F6) which might represent another layer of fine grained deposits, sealing a subglacially formed surface. Like in the case of horizon A there is a broad channel-like feature (in the center of S2) which—in analogue to horizon A—might also be a subglacial meltwater channel. Again the setting can be interpreted as a basin fill during an older Termination after a major glaciation.

The character of the deepest part of the basin is completely different from the shallower sequences. From facies F2 a high energy environment such as braided river deposits, is inferred. Finckh et al. (1984) report such

seismic facies from the deepest sections of lake Zurich where borehole penetrated well sorted gravel. Also the deepest part of the basin is bounded by steep (up to 25°) flanks. Parts of the basin are probably of tectonic origin; main faults are oriented NW–SE (Fig. 7). It has to be highlighted that faulting did not affect the superposing infill from horizon B upward.

Interpretation regarding climatostratigraphy (Figs. 12, 13)

Three different coarsening-upward sequences, each with baselap structures, are evident. The uppermost sequence with deltaic sediments on top of subglacial till is regarded to display the sedimentary characteristics of a Termination

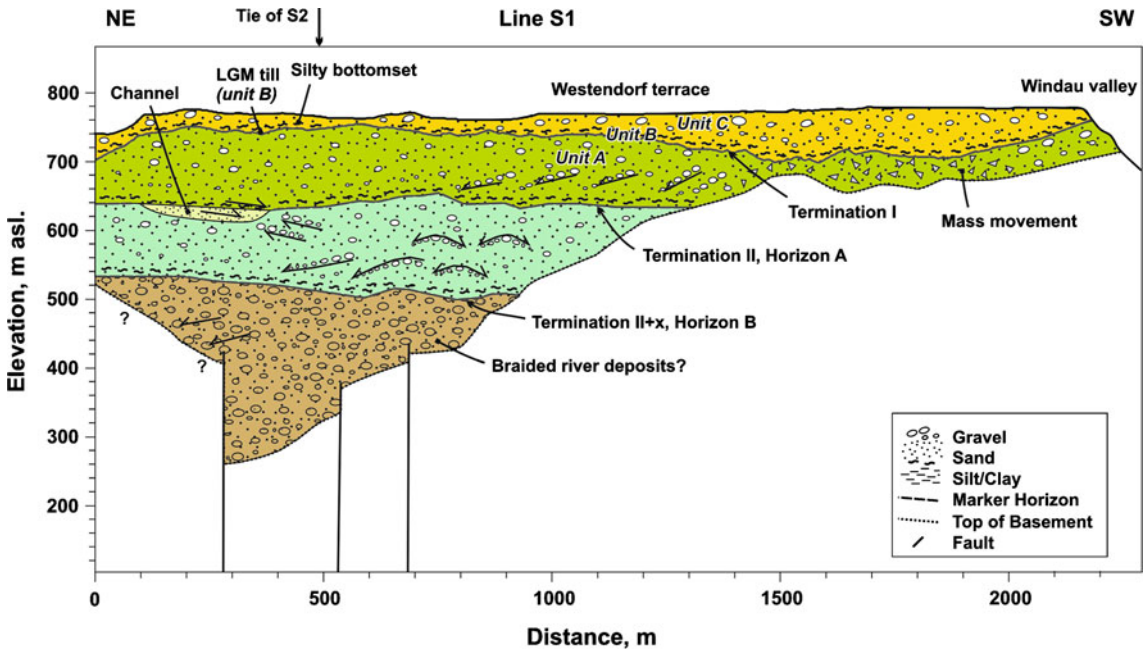

Fig. 12 Joint geological interpretation profile 1 (along S1 and G1)

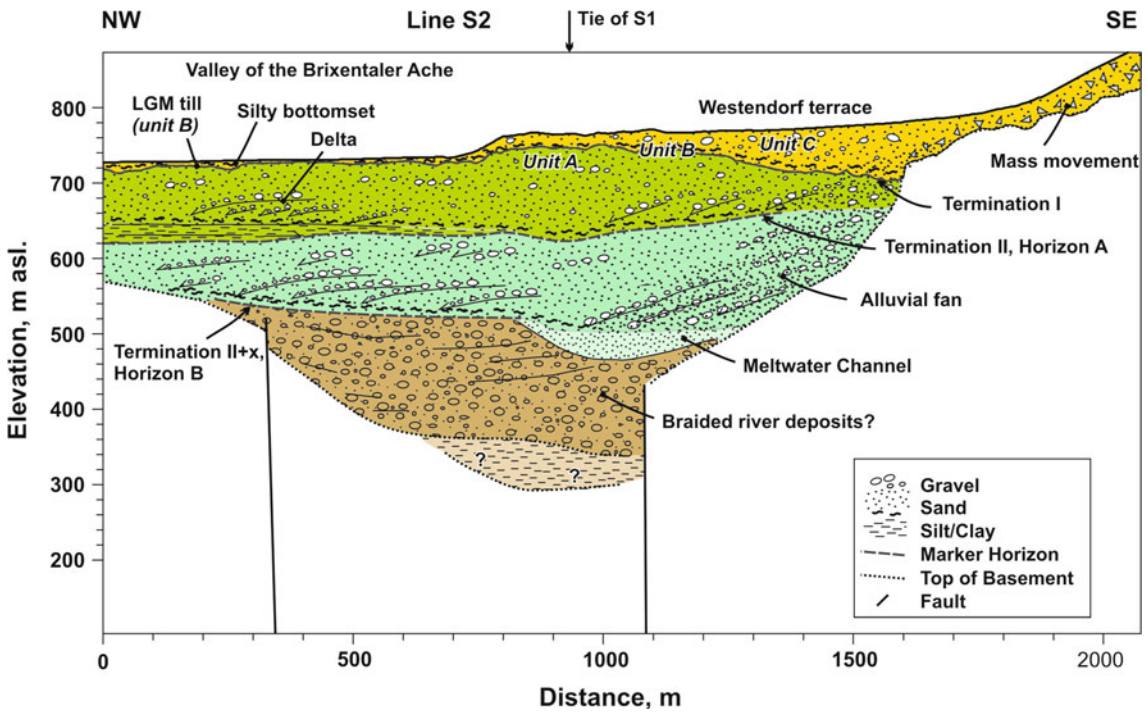

Fig. 13 Joint geological interpretation profile 2 (along S2 and G2)

in climatostratigraphy i.e. rapid deglaciation after a major glaciation (Broecker 1984). In this case the deposits represent the phase of early Lateglacial ice decay (Reitner 2007) at the beginning of Termination I after the LGM (Würmian Pleniglacial, MIS 2). The accommodation space of the ice dammed lakes of Termination I was the result of subglacial erosion during a complete ice infill of the Hopfgarten basin dominated by the Inn glacier and glacier flow through it. These pleniglacial conditions of the LGM differ substantially from that of the following phase, when the local glaciers of Windau and Kelchsau valley reached their Lateglacial Maximum Position just at the margin of the Hopfgarten basin (Figs. 3, 4; Reitner 2007). Below these documents of Termination I (MIS 2) the interpretation relies on a combination of surface and subsurface data. The next lower sequence is confined upward by the erosional base of the LGM till and downward by the prominent horizon A plane. The uppermost, outcropping part of the enclosed sedimentary succession resembles sediments of early Würmian age (MIS 5d-5a) according to the palynostratigrahic classification of the lignites (Reitner and Draxler 2002). Glaciation during the stadials MIS 5b and 5d was restricted and even smaller than the Lateglacial Maximum Position (Reitner 2007). Such a finding is in accordance with the paleoclimate model derived from palynological investigations of lacustrine sediments at Samerberg (35 km north of Hopfgarten; Grüger 1979, Fig. 1) and also with an ice-free Inn valley around Innsbruck from MIS 5c to MIS 5a (Spötl and Mangini 2006). The following deltaic structures well below modern valley floors of the Brixentaler Ache are regarded to document a phase of valley infill after a major glaciation, which again created an accommodation space for the subsequent sedimentation. Even though indications for MIS 5e, the Eemian interglacial, are missing in the Hopfgarten basin, it is obvious and in consensus with the various Eastern alpine locations (Grüger 1979; Drescher-Schneider 2000; Draxler 2000) to attribute those characteristic sediments to Termination II, following the Rissian (MIS 6). This penultimate glaciation, which lasted from 185 to 130 kyr BP (Spötl et al. 2007) according to speleothem data, was more extended in the Alpine foreland than the LGM (Penck and Brückner 1909). However, no chronological constraints for the climax of the Rissian glaciation in the Eastern Alps, and thus the presence of pleniglacial conditions in the Hopfgarten basin exist so far.

For the next lower sequence, between the limits of the horizons A and B, with again indications of downlap structures typical for deltaic infill, no chronostratigraphic information is available. Strata lie in sequence above sediments of a Termination. However, it is supposed that another sequence also lies underneath Termination II, which must be older than Rissian age. If we consider that longitudinal valleys like the Inn valley not only controlled the accelerated ice build-up, but also the principal extent of the glaciers there (van Husen 2000, 2004), then pleniglacial conditions in the Hopfgarten basin most probably took place only during phases of major glaciations. Moreover, as the onset of those major events in the Alpine realm occurred from MIS 22 (0.87 Ma) onwards (Muttoni et al. 2003, 2007), such pleniglacial conditions maybe reached only during phases of "excess ice" within the last 800 kyr (Raymo 1997) and thus within the middle and upper Pleistocene (van Husen 2000, 2004). These are beside the documented MIS 2 (Würmian-Pleniglacial) and the indirectly proved MIS 6 (Rissian-Pleniglacial), MIS 10, MIS 12 and MIS 16 (Raymo 1997). Thus, like in the Samerberg area (Jerz 1983; Grüger 1983), the most prominent glacial erosion may have occurred before the Holstein-interglacial (MIS 11), during MIS 12 followed by basin infill starting with Termination V.

The lowermost sequence covering the basement and beyond the Termination II + x (horizon B) reveals a completely extraordinary position within the whole sedimentary inventory of the Hopfgarten basin. Indications of downlap structures typical for deltaic infill of a glacially overdeepened basin like in the sequences above are missing. According to previous arguments it may document very coarse grained deposits, which are displaced by vertical faults linked to the Inntal fault system (Fig. 7). According to such a setting we cannot even exclude Oligocene sediments, and thus pendants to the Oberangerberg formation (Ortner and Stingl 2001) consisting of braided river deposits of the paleo Inn river or even the coarse-grained alluvial fan deposits of the Lengergraben member (Häring formation, Ortner and Stingl 2001) of the Inn valley.

Implications for glacier flow previous to the LGM

The preservation of sedimentary documents of terminations older than Termination I, as well as the obvious reduction in overdeepening/subglacial erosion in the Hopfgarten basin during subsequent glaciations, raises the question of its reasons: is this feature the expression of randomly occurring processes in the sense of intrinsic variations of the glacier flow including its subglacial meltwater flow? Or does the sequence reflect a systematical change in terms of e.g. different duration of glacial climaxes or topographical evolution?

It is a fact that the geometry of the ersosional surfaces of the LGM in the whole basin and of the two older glaciations in the Westendorf area do not show a major impact of linear subglacial meltwater action in the sense of "tunnel valleys", whose position might change even within glaciations due to internal re-organisations of the subglacial drainage (e.g. Kristensen et al. 2007).

Based on findings in inneralpine valleys for the last glacial cycle (van Husen 2000, 2004), every advancing glacier had in its proglacial areas a more or less thick sequence of unfrozen unlithified sediments due to climatically steered aggradation before the climax of the respective glaciation. Such an assumption is also in accordance with the known course of climatic detoriation showing long trends of cooling/glacier growth towards a glacial climax (Raymo 1997). Hence, no principal difference in the subglacial hydraulic conditions promoting or impeding glacial erosion in the sense of pore water changes affecting sediment deformation and evacuation (Menzies 1995; Boulton 2007) can be deduced between the various glaciations.

Differences in the duration of the respective glacial culminations during which the Hopfgarten basin was subjected to ice flow and thus erosion, might be responsible as well. It has to be emphasized that such data for pleniglacial conditions of the Würmian vary between 3 kyrs (Preusser 2004) and more than 5 kyrs (Monegato et al. 2007). Equivalents of the older glaciations are missing completely for the Alpine region.

Another plausible reason for the remarkable differences in subglacial overdeepening might be the regional ice flow setting. If the impeded ice flow in the Hopfgarten basin is considered to be the reason for the minor erosion during the LGM (s. Fig. 6), then a little change in this complex paleogeographic situation might have had a big impact. The accumulation area of the Inn glacier is regarded to have remained more or less the same throughout the last 800 kyrs (middle–upper Pleistocene) as the Inn glacier flow was determined by the existing free river drainage. In contrast, the dominance of the Achen glacier, which was responsible for the relatively early ice flow blockade towards the east during the LGM, relied mostly on the ice influx from the mountain range Hohen Tauern via the Pass Thurn (1,274 m asl.; Reitner 2005; Fig. 14a). Moreover, the impact of the higher elevated transfluence routes (*A*, *B*, *C* in Fig. 2) towards the Windau and Kelchsau valley also impeded the passage of Inn ice towards the east in a later phase of the LGM (Fig. 14b). From the morphology of all of these coles, especially that of Pass Thurn, a substantial lowering of the altitude due to abrasion by a fast ice flow, can be inferred. Additionally, in such a narrowing of glacier flow crevasses most probably occurred on its relatively steepened surface, which enabled a fluctuating meltwater flux down to the base. Thus, associated variations of hydraulic pressure should have promoted very effective bedrock erosion by quarrying too (Hooke 1991). If we consider

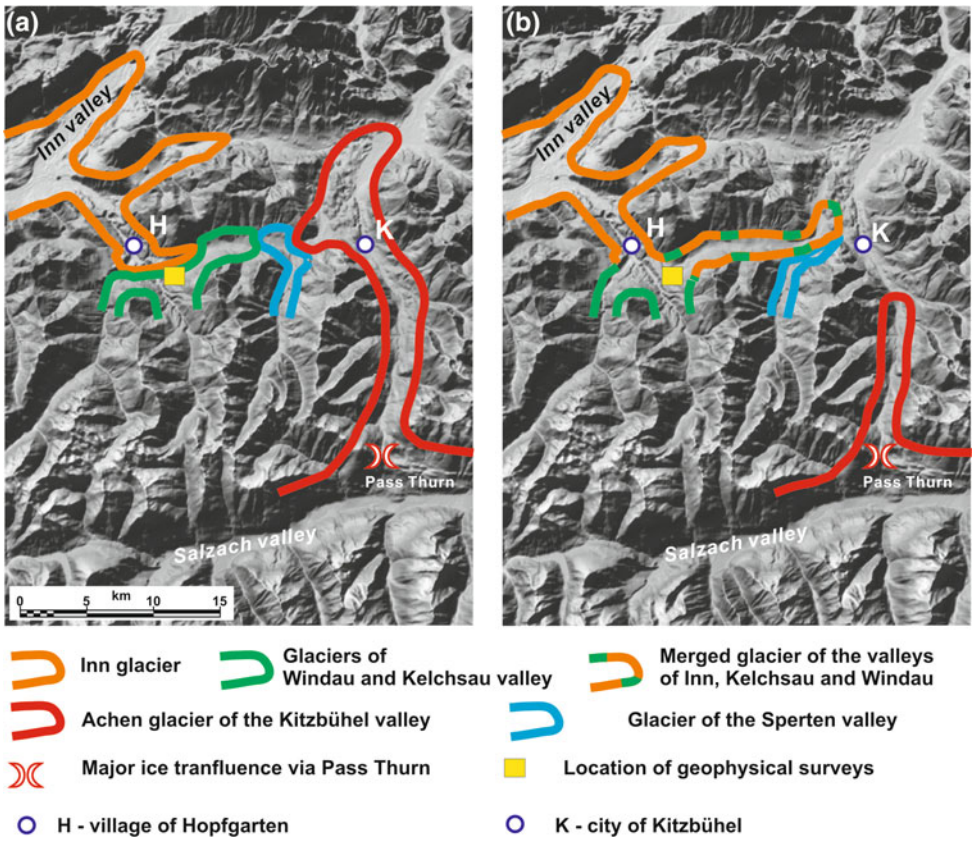

Fig. 14 Schematic paleogeographical sketch map of the LGM ice build-up situation (**a**) and of the relative oldest glaciation (**b**) causing overdeepening in the Hopfgarten basin. **a** The situation when overdeepening in the basin of Hopfgarten stopped due to the blockade by the Achen glacier, which at that time already got an strong supply via the low transfluence route of Pass Thurn from the Salzach glacier. **b** In contrast during an older glaciations (before Termination II + *x*), the Achen glacier was not able to do imped glacier flow towards east due to a relatively high elevated ice transfluence route, which did not allow such a strong inflow of ice from the south as it had occurred at the beginning of the LGM. Such a paleogeographic situation allowed unimpeded advance of Inn and tributary glacier towards east resulting in substantial overdeepening during this phase

these processes, erosion rate in such a constrained situation might have been at least in the upper range of the data with 10–100 mm/year reported for fast flowing glaciers (Hallet et al. 1996). In such a complex setting higher elevated transfluence routes previous to the LGM, especially in the source area of the Achen glacier, led to a relatively unimpeded inflow of Inn ice towards the east and maybe to a substantial extent of the Inn glacier domain in this direction (Fig. 14). This situation most probably had a major effect on overdeepening especially in the ice build-up phase of each glaciation. Thus, the preservation of sediments of older glacial cycles in the Hopfgarten basin is regarded to reflect the subsequent lowering of transfluence passes, especially due to subglacial erosion during the, respectively, previous glaciation. In this respect, a systematic change in morphology and a link between surface and subsurface topographic evolution is evident.

Conclusions

Based on the interpretation of the seismic survey, formation of the Hopfgarten basin seems to be a result of fault-related tectonic subsidence linked to the Inn fault system occurring most probably during the Miocene. The lowermost basin fill may represent Neogene and perhaps older sediments, and shows similarities to deposits of the nearby Inn valley. In the Inn valley a recent drilling (at Kramsach, Fig. 1) and a re-assessment of seismic data show Oligocene sediments as the predominant infill of the overdeepened valley (discussion in Preusser et al. 2010). Hence, the example of the Hopfgarten basin also shows the significance of Miocene tectonics shaping the subsurface bedrock topography along overdeepened, longitudinal valleys, which has so far been underestimated within the Eastern Alps.

The three documented Pleistocene sequences of the Hopfgarten basin all reveal a pattern of subglacial erosion, followed by glaciolacustrine to -deltaic sedimentation. The upper two cycles of this sedimentation are well constrained in time, having occured during the Würmian-pleniglacial (MIS 2) followed by Termination I and during the Rissian-pleniglacial (MIS 6) followed by Termination II. The timing of the first documented glacial shaping of the basin remains elusive. As the onset of major glaciations in the Alps occurred from 0.87 Ma onwards (Muttoni et al. 2003, 2007) further pleniglacial conditions most probably took place during the middle Pleistocene glacial events of MIS 10, 12 or 16 according to Raymo (1997). When compared to the situation of Samerberg (Jerz 1983; Grüger 1983), the oldest recorded glacial event at Hopfgarten may be that of MIS 12, which is correlated with one major glacial event in the Alps (e.g. Raymo 1997, van Husen 2000, 2004) and followed by Termination V.

According to van Husen (2000, 2004), ice build-up and extent were controlled, at least from the middle Pleistocene onwards, by a large scale drainage system of dominant, E–W trending, longitudinal valleys which resulted from Miocene continental extrusion (Frisch et al. 1998). This hypothesis is supported by the reconstruction of events in the Hopfgarten basin indicating an early inflow of the Inn glacier at LGM. The model of ice flow during this time describes an early mutual blockade of glaciers and a major E–W trending topographic barrier, resulting in only limited subglacial erosion most probably during the early phase of ice build-up. However, this model is challenged by the existence of major overdeepenings from the two older glaciations. We assume that the trend towards reduced glacial erosion mirrors a more general trend in the evolution of the highly dissected Eastern Alpine landscape. This is the lowering of passes and cols due to action of ice transfluences from the E–W trending longitudinal valleys towards the north, typical for glacier flow independent from the drainage pattern during pleniglacial conditions.

Our model for a dynamic evolution of morphology presents an inverse relationship between the shaping of the surface and the subsurface and may only hold for a restricted area. However, this non-static view on glacier constellation and its change through time can explain the occurrence of unexpected overdeepenings or changes in erratic clast content elsewhere in dissected, formerly glaciated, Alpine landscapes with complex ice flow patterns and history (e.g. North American Cordilleran, Stumpf et al. 2000).

Further studies linking surface geology and geophysical data, such as seismic stratigraphy, are needed to unravel the landscape evolution of the Eastern Alps. They must be accompanied by high quality core drillings in order to test the supposed lithostratigraphic and chronostratigraphic framework.

Acknowledgments The interpretation of the surface data gratefully benefited from many discussions with Dirk van Husen. We are also indebted to Ilse Draxler for palynological investigations as well as to Alfred Gruber, Helmut Heinisch and Hugo Ortner for their helpful remarks and suggestions on the tectonic evolution. We appreciate the careful improvements of the whole text by Nicole Kemp, Doris Reischenbacher and some of its parts by Sebastian Pfleiderer and John Menzies. The efforts of Birgit Jochum, Gerhard Bieber and Anna Ita during the geoelectrical survey are gratefully acknowledged. Information provided by Gert Gasser and Christian Schmid on the subcrop situation in the Inn valley were very helpful. Finally, we thank the community of Westendorf for the permission to publish the data of the seismic survey and for organizational support during the geoelectric survey. The authors are indebted to Sven Lukas, Bernhard Salcher and Michael Schnellmann for their constructive comments on an earlier version of the manuscript.

References

Alley, R. B., Lawson, D. E., Larson, G. J., Evenson, E. B., & Baker, G. S. (2003). Stabilizing feedbacks in glacier-bed erosion. *Nature, 424*, 758–760.

Ampferer, O., & Ohnesorge, T. (1918). *Rattenberg. Geologische Spezialkarte der Österreichisch-Ungarischen Monarchie*, 1:75.000, Blatt 5048, Vienna: Geologische Reichsanstalt.

Bates, R. L., & Jackson, J. A. (Eds.) (1987). *Glossary of Geology*. (3rd ed., p. 788), Alexandria, Virginia: American Geological.

Benn, D. I., & Evans, D. J. A. (1998). *Glaciers and glaciation* (p. 734). London: Arnold.

Boulton, G. S. (2007). Glaciers and their coupling with hydraulic and sedimentary processes. In: , P. G. Knight (Ed.), *Glacier science and environmental change*. 3–22.

Broecker, W. S. (1984). Terminations, in Milankovitch and climate. Part 2. In: Berger, A., Reidel D. (Eds.) (pp. 687–698), Norwell, Mass.

Brown, A. R. (2004). *Interpretation of three-dimensional seismic data* (6th ed.). Tulsa: AAPG Memoir 42.

Büker, F., Green, A. G., & Horstmeyer, H. (1998). Shallow seismic reflection study of a glaciated valley. *Geophysics, 63*, 1395–1407.

Burgschwaiger, E., & Schmid, C. (2001). Seismostratigrafische Untersuchungen der Talfüllung des oberen Trauntales bei Ebensee. In: C. Hammerl, W. Lenhardt, R. Steinacker, & P. Steinhauser (Eds.), *Die Zentralanstalt für Meteorologie und Geodynamik* (pp. 792–797). Graz: Leykam.

Clearbout, J. (1976). *Fundamentals of geophysical data processing*. New York: McGraw-Hill.

Draxler, I. (2000). Pollenanalytische Untersuchungen der schieferkohleführenden Sedimentfolge von Nieselach bei St. Stefan im unteren Gailtal, Kärnten. Mitteilungen der Kommission für Quartärforschung Österreichische Akademie der Wissenschaften *12*, 155–179, Vienna.

Dreimanis, A. (1988). Tills: Their genetic terminology and classification. In R. P. Goldthwait & C. L. Matsch (Eds.), *Genetic classification of glacigenic deposits: Final report of the Commission on Genesis and Lithology of Glacial Quaternary Deposits of the International Union of Quaternary Research (INQUA)* (pp. 17–83). Rotterdam: Balkema.

Drescher-Schneider, R. (2000). Die Vegetations- und Klimaentwicklung im Riß/Würm-Interglazial und im Früh- und Mittelwürm in der Umgebung von Mondsee—Ergebnisse der pollenanalytischen Untersuchungen.- Mitteilungen der Kommission für Quartärforschung Österreichische Akademie der Wissenschaften 12, 39–92, Vienna.

Evans, D. J. A., & Benn, D. I. (2004). Facies description and the logging of sedimentary exposures. In: Evans, D. J. A., Benn, D. I. (Eds.), *A practical guide to the study of glacial sediments*. 11–50, Arnold.

Evans, D. J. A., Phillips, E. R., Hiemstra, J. F., & Auton, C. A. (2006). Subglacial till: Formation, sedimentary characteristics and classification. *Earth-Science Reviews, 78*, 115–176.

Eyles, N., Eyles, H. C., & Miall, A. D. (1983). Lithofacies types and vertical profile models; an alternative approach to the description and environmental interpretation of glacial diamict and diamictite sequences. *Sedimentology, 30*, 393–410.

Finkh, P., Kelts, K., & Lambert, A. (1984). Seismic stratigraphy and bedrock forms in perialpine lakes. *Bulletin Geological Society of America, 95*, 1118–1128.

Fliri, F. (1973). Beiträge zur alpinen Würmvereisung: Forschungen am Bänderton von Baumkirchen (Inntal, Nordtirol).- Zeitschrift für Geomorphologie, N. F. (Suppl 16, 1–14), Berlin, Stuttgart.

Frisch, W., Kuhlemann, J., Dunkl, I., & Brügel, A. (1998). Palinspastic reconstruction and topographic evolution of the Eastern Alps during late tertiary tectonic extrusion. *Tectonophysics, 297*, 1–15.

Grenerczy, G., Sella, G., Stein, S., & Kenyeres, A. (2005). Tectonic implications of the GPS velocity field in the northern Adriatic region. *Geophysical Research Letter, 32*, L16311.

Gruber, W., Morawetz, R., & Schramm, J. M. (2004). *Reflexionsseismik Westendorf. Unpubl. report* (p. 12). Leoben: Joanneum Research.

Gruber, A., Strauhal, T., Prager, C., Reitner, J. M., Brandner, R., & Zangerl, C. (2009). Die "Butterbichl-Gleitmasse—eine große fossile Massenbewegung am Südrand der Nördlichen Kalkalpen (Tirol, Österreich). *Bulletin für angewandte Geologie, 14/1+2*, 103–134.

Gruber, W., & Weber, F. (2004). Ein Beitrag zur Kenntnis des glazial übertieften Inntals westlich von Innsbruck. *Sitzungsberichte Abteilung I der Österreichischen Akademie der Wissenschaften, 210*(2003), 3–30.

Grüger, E. (1979). Spätriss, Riss/Würm und Frühwürm am Samerberg in Oberbayern—ein vegetationsgeschichtlicher Beitrag zur Gliederung des Jungpleistozäns. *Geologica Bavarica, 80*, 5–64, Munich.

Grüger, E. (1983). Untersuchungen zur Gliederung und Vegetationsgeschichte des Mittelpleistozäns am Samerberg in Oberbayern. *Geologica Bavarica, 84*, 21–40.

Hallet, B., Hunter, L., & Bogenc, J. (1996). Rates of erosion and sediment evacuation by glaciers: A review of field data and their implications. *Global and Planetary Change, 12*, 213–235.

Heinisch, H. (2003). Bericht 2002 über geologische Aufnahmen im Paläozoikum der Nördlichen Grauwackenzone und in der Gaisbergtrias auf Blatt 121 Neukirchen am Großvenediger. *Jahrbuch der Geologischen Bundesanstalt 143*, 476, Vienna.

Heinisch, H. (2005). Bericht 2004 über geologische Aufnahmen im Paläozoikum der Nördlichen Grauwackenzone und im angrenzenden Permoskyth auf den Blättern 120 Wörgl und 121 Neukirchen am Großvenediger. *Jahrbuch der Geologischen Bundesanstalt, 145*, 330–332. Vienna.

Heinisch, H., & Panwitz, C. (2007). Bericht 2006 über geologische Aufnahmen auf ÖK 121 Neukirchen a.G. im Paläozoikum der Nördlichen Grauwackenzone. *Jahrbuch der Geologischen Bundesanstalt, 147*, 654–656. Vienna.

Hooke, R. L. (1991). Positive feedbacks associated with erosion of glacial cirques and overdeepenings. *Geological Society of America Bulletin, 103*, 1104–1108.

Jerz, H. (1983). Die Bohrung Samerberg 2 östlich Nußdorf am Inn. *Geologica Bavarica, 84*, 6–16.

Jones, A. P., Tucker, M. E., & Hart, J. K. (1999). Guidelines and recommendations. In: Jones, A. P., Tucker, M. E.,& Hart, J. K. (Eds.), *The description and analysis of quaternary stratigraphic field sections. Technical guide 7*, (27–62), London: Quaternary Research Association.

Jopling, A. V., & Walker, R. G. (1968). Morphology and origin of ripple-drift cross-lamination, with examples from the Pleistocene of Massachusetts. *Journal of Sedimentary Petrology, 84*(4), 971–984.

Keller, B. (1996). Lithofazies-Codes für die Klassifikation von Lockergesteinen. *Mitteilungen der Schweizerischen Gesellschaft für Boden- und Felsmechanik, 132*, 5–10.

Klasen, N., Fiebig, M., Preusser, F., Reitner, J. M., & Radtke, U. (2007). Luminescence dating of sediments from the Tyrolean Alps, Austria, and implications for the reconstruction of ice dynamics during the last glaciation. *Quaternary International, 164–165*, 21–32.

Kristensen, T. B., Huuse, M., Piotrowski, J. A., & Clausen, O. R. (2007). A morphometric analysis of tunnel valleys in the eastern North Sea based on 3D seismic data. *Journal of Quaternary Science, 22*, 747–825.

Menzies, J. (1995). Hydrology of Glaciers. In J. Menzies (Ed.), *Modern glacial environments: Processes, dynamics and sediments* (pp. 197–239). Oxford: Butterworth-Heinmann.

Miall, A. D. (1996). *The Geology of fluvial deposits*. (582 p), Springer.

Monegato, G., Ravazzi, C., Donegana, M., Pini, R., Calderoni, G., & Wick, L. (2007). Evidence of a two-fold glacial advance during the last glacial maximum in the Tagliamento end moraine system (Eastern Alps). *Quaternary Research, 68*, 284–302.

Mostler, H. (1993). Erkundung von Kies- und Sandvorkommen in Tirol (Phase II: Detailuntersuchungen). Bund/Bundesländer-Rohstoffprojekt T-A-034/92, Endbericht. 160 p. Unpubl. report (archive of the Geological Survey of Austria).

Muttoni, G., Carcano, C., Garzanti, E., Ghielmi, M., Piccin, A., Pini, R., et al. (2003). Onset of major Pleistocene glaciations in the Alps. *Geology, 31*, 989–992.

Muttoni, G., Ravazzi, C., Breda, M., Laj, C., Kissel, C., Mazaud, A., et al. (2007). Magnetostratigraphy of the Leffe lacustrine succession (Southern Alps, Italy): evidence for an intensification of glacial activity in the Alps at Marine Isotope Stage 22 (0.87 Ma). *Quaternary Research, 67*, 161–173.

Nitsche, F. O., Monin, G., Marillier, F., Graf, H., & Ansorge, J. (2001). Reflection seismic study of Cenozoic sediments in an overdeepened valley of northern Switzerland: The Birrfeld area. *Eclogae Geologicae Helveticae, 94*, 363–371.

Oldenburg, D., & Li, Y. (1994). Inversion of induced polarization data. *Geophysics, 59*, 1327–1341.

Ortner, H., & Stingl, F. (2001). Facies and basin development of the Oligocene in the Lower Inn Valley, Tyrol/Bavaria. In: W. E. Piller & M. W. Rasser (Eds.), *Paleogene of the Eastern Alps*, *Österreichische Akademie der Wissenschaften, Schriftenreihe der erdwissenschaftlichen Kommission 14*, (153–197), Vienna.

Palmer, D. (1980). *The generalized reciprocal method of seismic refraction interpretation* (p. 104). Tulsa: Society of. Exploration Geophysicists.

Penck, A., & Brückner, E. (1909). *Die Alpen im Eiszeitalter. Bd. I-III* (p. 1199). Leipzig: Tauchnitz.

Pestal, G., Hejl, E., Egger, H., van Husen, D., Linner, M., Mandl, G., et al. (2004). *Geologische Karte von Salzburg 1:200000*. Vienna: Geologische Bundesanstalt.

Pfiffner, O. A., Heitzmann, P., Lehner, P., Frei, W., Pugin, A., & Felber, M. (1997). Incision and backfilling of Alpine valleys: Pliocene, Pleistocene and Holocene processes. In: O. A. Pfiffner, P. Lehner, P. Heitzmann, S. Mueller & A. Steck (Eds.), *Deep Structure of the Swiss Alps: results of NRP 20*. Birkhäuser Basel, 265–288.

Poscher, G. (1993). *Neuergebnisse der Quartärforschung in Tirol.- Arbeitstagung der Geologischen Bundesanstalt 1993*, 7–27, Vienna.

Postma, G. (1990) Depositional architecture and facies of river and fan deltas: A synthesis. In: A. Colella & D. P. Prior (Eds.), *Coarse-grained deltas*, *Special Publications 27th International Association of Sedimentologist, 10*, 13–27.

Preusser, F. (2004). Towards a chronology of the Late Pleistocene in the northern Alpine Foreland. *Boreas, 33*, 195–210.

Preusser, F., Reitner, J. M., & Schlüchter, C. (2010). Distribution, geometry, age and origin of overdeepened valleys and basins in the Alps and their foreland. *Swiss Journal of Geoscience* (this volume). doi:10.1007/s00015-010-0044-y.

Raymo, M. E. (1997). The timing of major climatic terminations. *Paleooceanography, 12*, 577–585.

Reitner, J. M. (2005). Quartärgeologie und Landschaftsentwicklung im Raum Kitzbühel—St. Johann i.T. – Hopfgarten (Nordtirol) vom Riss bis in das Würm-Spätglazial (MIS 6-2). PhD-Thesis, 190 p., University of Vienna.

Reitner, J. M. (2007). Glacial dynamics at the beginning of Termination I in the Eastern Alps and their stratigraphic implications. *Quaternary International, 164–165*, 64–84.

Reitner, J. M. (2008). Bericht 2006/2007 über geologische Aufnahmen im Quartär auf den Blättern 120 Wörgl und 121 Neukirchen am Großvenediger bzw.auf UTM-Blatt 3213 Kufstein. Jahrbuch der Geologischen Bundesanstalt, 148.2, Wien. 248–254, Vienna.

Reitner, J. M., & Draxler, I. (2002). Die klimatisch-fazielle Entwicklung vor dem Würm - Maximum im Raum Kitzbühel - St.Johann - Hopfgarten (Nordtirol/Österreich). *Terra Nostra, 2002*(6), 298–304.

Sasaki, Y. (1992). Resolution of resistivity tomography inferred from numerical simulation. *Geophysical Prospecting, 40*, 453–464.

Schlüchter, C. (1983). Die Bedeutung der angewandten Geologie für die eiszeitgeologische Forschung in der Schweiz. *Physische Geographie II*, 59–72.

Schulz, O., & Fuchs, W. (1991). *Kohle in Tirol. Archiv für Lagerstättenforschung*, Geologische Bundesanstalt 13, 123–213, Vienna.

Slotnik, M. M. (1936). On seismic computations, with applications I. *Geophysics, 1*, 2–22.

Smith, A. M., Murray, T., Nicholls, K. W., Makinson, K., Aðalgeirsdóttir, G., Behar, A. E., et al. (2007). Rapid erosion, drumlin formation, and changing hydrology beneath an Antarctic ice stream. *Geology, 35*, 127–130.

Spötl, C., Holzkämper, S., & Mangini, A. (2007). The Last and the Penultimate Interglacial as recorded by speleothems from a climatically sensitive high-elevation cave site in the Alps. In: F. Sirocko, M. Claussen, T. Litt, & Sánchez-Goñi M. F. (Eds.) *The Climate of Past Interglacials—Developments in Quaternary Science Series 7*, (pp. 471–491) Oxford: Elsevier.

Spötl, C., & Mangini, A. (2006). U/Th age constraints on the absence of ice in the central Inn Valley (Eastern Alps, Austria) during Marine Isotope Stages 5c to 5a. *Quaternary Research, 66*, 167–175.

Stumpf, A. J., Broster, B. E. & Levson, V. M. (2000). Multiphase flow of the late Wisconsinan Cordilleran ice sheet in Western Canada. *Geological Society of America Bulletin, 112*, 1850–1863.

van Husen, D. (1979). Verbreitung, Ursachen und Füllung glazial übertiefter Talabschnitte an Beispielen aus den Ostalpen. *Eiszeitalter und Gegenwart, 29*, 9–22.

van Husen, D. (1987). *Die Ostalpen in den Eiszeiten* (p. 24). Vienna: Veröffentlichung der Geologischen Bundesanstalt 2.

van Husen, D. (2000). Geological processes during the quaternary. *Mitteilungen der Österreichischen Geologischen Gesellschaft, 92*(1999), 135–156. Vienna.

van Husen, D. (2004). Quaternary glaciations in Austria. In: J. Ehlers, P. L. Gibbard (Eds.), *Quarternary Glaciations—Extent and Chronology. Developments in Quaternary Science 2, Part I*: Europe, 401–412.

van Rensbergen, P., de Batist, M., Beck, C. H., & Chapron, E. (1999). High-resolution seismic stratigraphy of glacial to interglacial fill of a deep glacigenic lake: Lake Le Bourget, Northwestern Alps, France. *Sedimentary Geology 128*, 99–129.

Weber, F., Schmid, C., & Figala, G. (1990). Vorläufige Ergebnisse Reflectionsseismischer Messungen im Quartär des Inntals/Tirol. *Zeitschrift für Gletscherkunde und Glazialgeologie 26*(2), 121–144.

Wildi, W. (1984). Isohypsenkarte der quartären Felstäler in der Nord- und Ostschweiz, mit kurzen Erläuterungen. *Eclogae geologicae Helvetiae, 77*, 541–551.

Yilmaz, O. (1987). *Seismic data processing* (p. 526). Tulsa: SEG.

Zailer, V. (1910). Die diluvialen Torfkohlenlager von Hopfgarten. *Zeitschrift für Moorkultur und Torfverwertung, 8*, 267–281.